



Cite this: *Soft Matter*, 2025,  
21, 1603

Received 2nd December 2024,  
Accepted 5th February 2025

DOI: 10.1039/d4sm01430h

[rsc.li/soft-matter-journal](http://rsc.li/soft-matter-journal)

## 1. Introduction

Soft materials such as elastomers and hydrogels, feature a three-dimensional crosslinked polymer network that provides exceptional stretchability and elasticity.<sup>1–3</sup> These mechanical properties endow soft materials with capabilities such as energy dissipation,<sup>3</sup> adaptability to changing environments,<sup>4</sup> biocompatibility,<sup>5</sup> and nonlinear mechanical responsiveness.<sup>6</sup> Unlike rigid materials, soft materials can undergo extensive deformation while maintaining structural integrity, making them suitable for diverse applications stretchable electronics,<sup>7–9</sup> soft robotics,<sup>10–13</sup> and biomedical devices.<sup>14–18</sup> However, such applications subject soft materials to challenging conditions, including load-bearing conditions,<sup>19,20</sup> cyclic loading environments,<sup>21</sup> or damage-prone situations.<sup>22</sup> To ensure consistent and reliable performance under these conditions, soft materials require enhanced mechanical performance.

The mechanical properties of soft materials stem from entropic elasticity, which limits energy dissipation and makes the material vulnerable to fracture.<sup>23–25</sup> Researchers have developed network designs that increase the plastic zone size to improve energy dissipation and enhance fracture resistance.<sup>26–28</sup> However, this approach inevitably compromises elasticity, limiting the capacity of the material to recover its original state after

## Network design for soft materials: addressing elasticity and fracture resistance challenges

Yong Eun Cho,<sup>†,a</sup> Sihwan Lee,<sup>†,a</sup> Sang Jun Ma<sup>†,a</sup> and Jeong-Yun Sun  <sup>\*,ab</sup>

Soft materials, such as elastomers and gels, feature crosslinked polymer chains that provide stretchable and elastic mechanical properties. These properties are derived from entropic elasticity, which limits energy dissipation and makes the material susceptible to fracture. To address this issue, network designs that dissipate energy through the plastic zone have been introduced to enhance toughness; however, this approach compromises elasticity, preventing the material from fully recovering its original shape after deformation. In this review, we describe the trade-off between fracture resistance and elasticity, exploring network designs that overcome this limitation to achieve both high toughness and low hysteresis. The development of soft materials that are both elastic and fracture-resistant holds significant promise for applications in stretchable electronics, soft robotics, and biomedical devices. By analyzing successful network designs, we identify strategies to further improve these materials and discuss potential enhancements based on existing limitations.

deformation.<sup>3,29</sup> This inherent trade-off between fracture resistance and elasticity presents a significant challenge in developing soft materials that are simultaneously tough and elastic. Addressing this challenge requires a comprehensive understanding of how network design affects the mechanical properties of soft materials (Fig. 1).

The mechanical properties of soft materials are closely related to network design.<sup>30–32</sup> Enhancing the mechanical properties requires careful consideration of factors such as the type of polymer backbone,<sup>33</sup> the topology of chain connections,<sup>34–36</sup> molecular interactions between chains,<sup>37</sup> and interactions between polymers and solvents or additives.<sup>38,39</sup> To enhance the performance of soft materials, this review addresses network design strategies to resolve the trade-off between fracture resistance and elasticity. We begin by discussing the methods to characterize elasticity and fracture resistance, followed by an analysis of network designs that improve each property individually. The inherent trade-off is examined in detail, highlighting strategies that enable the simultaneous enhancement of toughness and elasticity. By analyzing successful network designs, we outline future directions and potential improvements based on current limitations.

## 2. Mechanisms and mechanical characterization of elasticity and fracture resistance in soft materials

Soft materials are characterized by their unique ability to undergo substantial deformations, even under small forces. Following such deformations, two key factors must be

<sup>a</sup> Department of Materials Science and Engineering, Seoul National University, Seoul 08826, Republic of Korea. E-mail: [lsihwan16@snu.ac.kr](mailto:lsihwan16@snu.ac.kr), [sang219@snu.ac.kr](mailto:sang219@snu.ac.kr), [jysun@snu.ac.kr](mailto:jysun@snu.ac.kr), [whdydams11@snu.ac.kr](mailto:whdydams11@snu.ac.kr)

<sup>b</sup> Research Institute of Advanced Materials (RIAM), Seoul National University, Seoul 08826, Republic of Korea

† These authors contribute to this work equally.



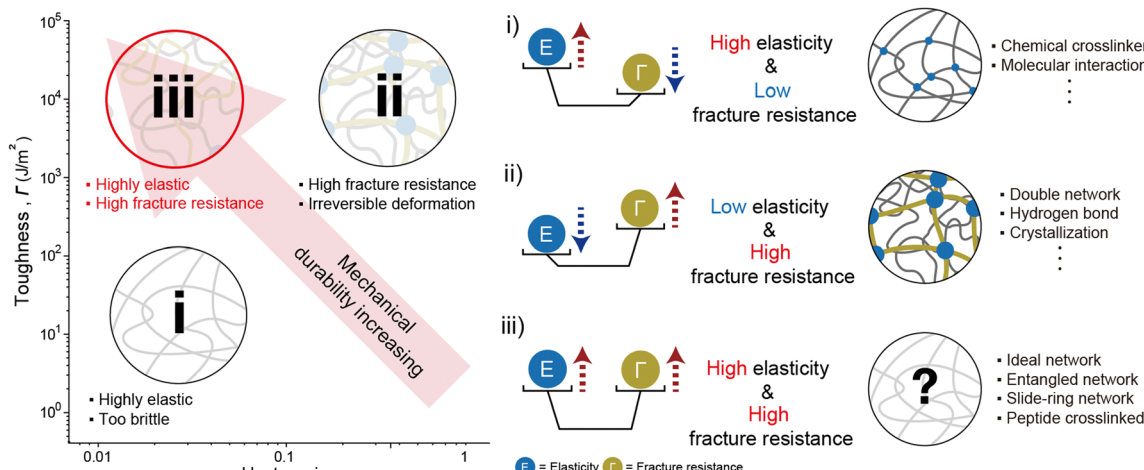


**Fig. 1** Trade-off between elasticity and fracture resistance in soft materials. (i) Soft materials that are generally elastic tend to have low fracture resistance and are therefore brittle. (ii) Soft materials with high fracture resistance lack elasticity, leading to irreversible deformation. To improve mechanical durability, it is essential to develop materials that are simultaneously elastic and fracture resistant. (iii) Network design enables the development of soft materials that can increase both elasticity and fracture resistance, overcoming the trade-off between these properties.

evaluated: (1) whether the material returns to its original shape upon removal of the external load, and (2) whether cracks propagate during deformation.<sup>40</sup> These can be characterized as elasticity and fracture resistance, respectively, and understanding both is crucial when evaluating soft materials.<sup>1,40,41</sup>

## 2.1 Brief overview

Elasticity describes the ability of a material to return to its original shape after being deformed by stress. This property is often evaluated through hysteresis, which quantifies the energy lost during cyclic loading and unloading of the material.<sup>42</sup> Materials exhibiting low hysteresis can recover elastically with high efficiency, making them suitable for repeated applications under consistent performance requirements.

Fracture resistance indicates the ability of a material to resist crack propagation during deformation. To quantify fracture resistance, toughness ( $\Gamma$ ) is introduced, which reflects the material's capacity to dissipate energy and prevent crack growth.<sup>43–45</sup> Materials with high toughness can withstand a variety of loads, enabling them to perform reliably across diverse conditions.

## 2.2 Origins of the elasticity-fracture resistance trade-off in soft materials

The mechanical performance of soft materials is primarily governed by entropic elasticity, which inherently restricts energy dissipation and leaves the material prone to fracture. To increase resistance to fracture, innovative network designs have been developed to expand the plastic deformation zone.<sup>3,29,46,47</sup> Energy dissipation in increasing plastic zone enhances fracture resistance significantly. However, indiscriminate increases in the plastic zone within the network have introduced unforeseen challenges, even in the absence of cracks. When strain is applied, internal plastic deformation within the network increases the hysteresis of the material,

even before fracture occurs. This relationship is distinctly observed in the Lake–Thomas model, one of the prominent approaches for explaining the fracture resistance of soft materials. An increase in cross-linking density in soft materials reduces fracture toughness. Simultaneously, higher cross-linking density decreases the distance between cross-linking points, resulting in enhanced entropic elasticity. A more detailed explanation of the Lake–Thomas model will be provided in the following section. Balancing these conflicting requirements of toughness and elasticity, as influenced by factors such as cross-linking density and energy dissipation, remains a critical challenge in the development of advanced soft materials (Fig. 2).

## 2.3 Theory of elasticity

The elasticity of soft materials composed of polymers is influenced by the conformation of polymer chains and molecular interactions. Due to their inherently long and flexible chains, polymers naturally adopt a coiled and disordered structure. This fundamental phenomenon can be explained from an entropic perspective, where entropic elasticity serves as a fundamental concept describing elasticity driven by the entropy of polymer chains.<sup>1,48,49</sup> When polymer chains stretched, these chains are forced into a more ordered conformation (low entropy state).<sup>1</sup> As soon as the external force is removed, they spontaneously return to their original, high-entropy, disordered state.

The number of conformations of the polymer chains,  $\Omega$  can be expressed as

$$\Omega \propto \exp\left(-\frac{3R^2}{2Nb_k^2}\right) \quad (1)$$

where  $R$  is the end-to-end distance,  $N$  is the number of segments in the chain, and  $b_k$  is the length of each segment. According to the Boltzmann relationship, the entropy  $S$  of the



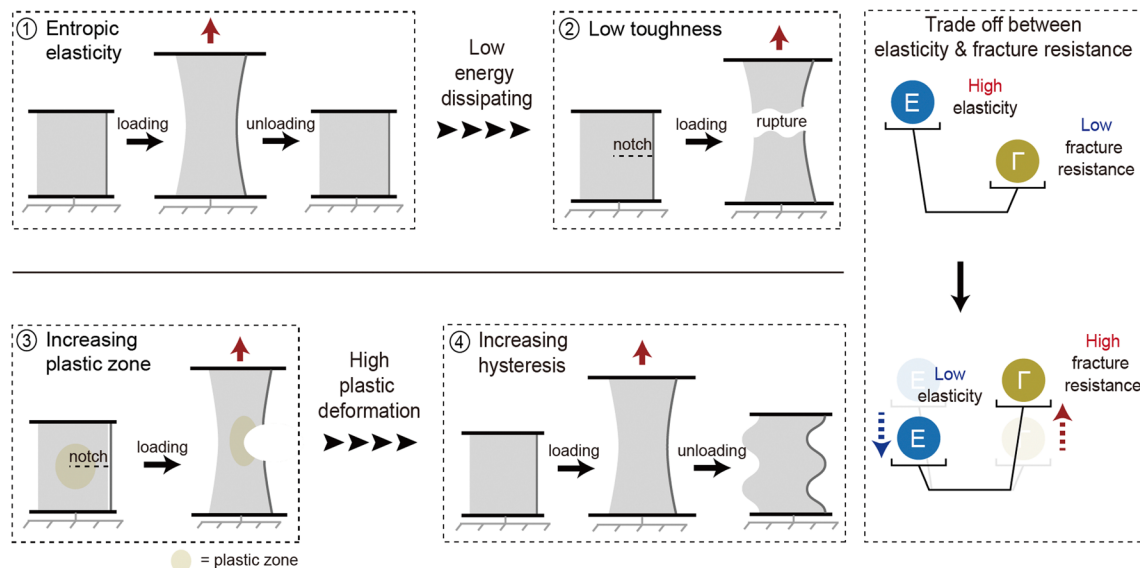


Fig. 2 Origin of elasticity and fracture resistance in soft materials. Soft materials possess intrinsic elasticity due to entropic elasticity, but their limited ability to dissipate energy results in low toughness. To address this issue, network designs that expand the plastic zone have been used to increase toughness; however, this also raises hysteresis.

polymer chain is

$$S = k_B \ln \Omega \approx -\frac{3k_B R^2}{2Nb_k^2} \quad (2)$$

where  $k_B$  is the Boltzmann constant. As  $R$  increases, the entropy  $S$  decreases, indicating that the system becomes more ordered as the polymer chain is stretched. The corresponding free energy  $F$  can be expressed as

$$F(R) = -TS \approx \frac{3k_B T}{2Nb_k^2} R^2 \quad (3)$$

where  $T$  is the temperature. This free energy function demonstrates that stretching a polymer chain requires energy. The restoring force  $f$  in entropic elasticity is derived from the free energy by taking its derivative with respect to the end-to-end distance  $R$ .

$$f = \frac{\partial F}{\partial R} = -T \left( \frac{\partial S}{\partial R} \right) = \frac{3k_B T}{Nb_k^2} R \quad (4)$$

Thus, when the polymer is extended, the number of possible conformations decreases, leading to a reduction in entropy<sup>1</sup> (Fig. 3a). The decrease in entropy creates a restoring force within the material. This entropic force strengthens with further stretching, working to return the chain to its original, disordered state. Such entropy-driven elasticity, known as entropic elasticity, is a fundamental characteristic of polymers. Besides entropic elasticity, introducing specific interactions within polymer networks can provide enthalpic contributions to enhance elasticity. Specifically, when external stress is applied, interactions dissociate, leading to an increase in energy as the system absorbs external energy. Subsequently reformation takes place, resulting in a decrease in energy. Swift and spontaneous transition from a high-energy state during dissociation to a lower-energy state during reformation drives

the ability of the materials to recover its original state. Therefore, molecular interactions can provide an additional restoring force, complementing the intrinsic elasticity of polymer chains.

#### 2.4 Testing methods for elasticity

The universal testing machine (UTM) is commonly used to measure the mechanical properties of soft materials, including tensile and compressive tests. To measure hysteresis, a loading–unloading curve is required. The energy applied during the loading process is called input energy ( $W_I$ ). The energy recovered by the material, known as elastic energy ( $W_E$ ), is the area beneath the unloading curve. The unrecovered energy, called dissipated energy ( $W_D$ ), is the area between the loading and unloading curves. These values satisfy the relationship  $W_D + W_E = W_I$ , and the energy dissipation ratio, calculated as  $\frac{W_D}{W_I} \times 100\%$ , quantifies hysteresis (Fig. 3b). A higher energy dissipation ratio indicates a reduced ability for the material to return to its original state after load removal. However, as soft materials exhibit viscoelastic properties, their behavior is time-dependent, making the loading rate an influential factor. Additionally, soft materials are generally capable of large deformations, meaning the extent of stretching has a considerable impact. Generally, the faster the loading rate and the greater the stretch, the higher the energy dissipation ratio.<sup>42</sup> Therefore, conducting experiments under identical conditions is crucial when comparing energy dissipation ratios. Residual stretch is a measure of elasticity, defined as the remaining stretch when the stress returns to zero after a material has been loaded and then unloaded.<sup>50</sup> Lower residual stretch values indicate better recovery to the original state, implying greater elasticity. Additionally, changes in the loading–unloading curve over multiple cycles can also be used to assess elasticity.<sup>40</sup> If the

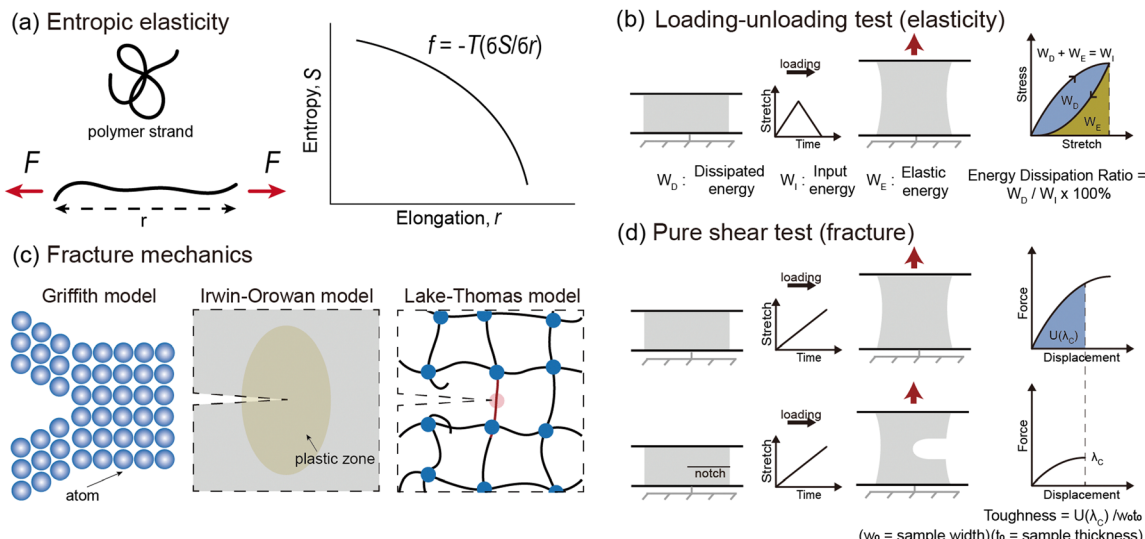


**Fig. 3** Theory and testing methods for elasticity and fracture resistance. (a) The elasticity of soft materials originates from entropic elasticity. Entropic elasticity arises from the tendency of disordered polymer chains to return to their original state of disorder after being aligned by an external force. (b) Loading–unloading test of soft materials to measure hysteresis. Stress–stretch curves of soft materials under cyclic loading with fixed stretch. Hysteresis (energy dissipation ratio) is defined as the ratio of the area between the loading and unloading curves ( $W_d$ ) to the area under the loading curve ( $W_i$ ). (c) Theoretical models from Griffith, Orowan–Irwin, and Lake–Thomas. The Griffith model is a theory that determines material fracture based on the energy required to create new surfaces. The Orowan–Irwin model suggests that additional energy dissipation through plastic deformation increases fracture resistance. In the Lake–Thomas model, stored energy in a chain is released by breaking the chain, thereby enhancing fracture resistance. (d) Pure shear test of soft materials to measure toughness ( $\Gamma$ ). Stress–stretch curves of soft material samples under monotonic loading with two samples: an unnotched sample and a notched sample.  $\Gamma$  is defined as the work done by the unnotched sample up to the critical stretch distance ( $\lambda_c$ ) of the notched sample,  $U(\lambda_c)$ , divided by the width ( $w_0$ ) and thickness ( $t_0$ ) of the un-notched sample.

curve remains consistent across many cycles, the material exhibits high elasticity. These measurements are essential for understanding a material's recovery ability after deformation, which is a critical factor in soft material design.

## 2.5 Theory of fracture mechanics

Fracture resistance, the energy required to propagate a crack, plays a pivotal role in determining the lifetime and mechanical durability of materials.<sup>40</sup> The ability to resist fracture depends on how effectively materials dissipate energy at both molecular and macroscopic levels. Intrinsically brittle materials, like silica glass, exhibit low fracture energy, as described by the Griffith model.<sup>51</sup> Ductile materials such as metals possess higher fracture energy, as explained by the Irwin–Orowan model,<sup>52,53</sup> which incorporates energy dissipation through plastic deformation near the crack tip. Crosslinked polymer networks achieve toughness through mechanisms specific to their structure. The Lake–Thomas model describes this toughness by considering energy dissipation along stretched covalent bonds within polymer chains, providing insights into the fracture resistance of polymers<sup>41</sup> (Fig. 3c).

In fracture mechanics, Griffith introduced a model in 1921 to calculate fracture energy based on the difference in energy before and after fracture.<sup>51</sup> According to Griffith, fracture occurs with the formation of two new surfaces; therefore, toughness can be expressed as

$$\Gamma = 2\gamma \quad (5)$$

where  $\gamma$  is the surface energy of the material. The Griffith model effectively describes brittle materials like glass, which fracture through atomic bond breakage. However, it underestimates the toughness of ductile materials and polymers, where additional fracture mechanics are present to increase toughness.

In the 1940s, G. Irwin and E. Orowan extended Griffith's model to include plastic deformation for ductile materials.<sup>52,53</sup> For such materials, local plasticity around the crack tip requires additional energy for fracture, enhancing fracture resistance. In metals, for example, a plastic zone forms near the crack tip, where atomic bonds release energy through deformation. Thus, considering the plastic zone, toughness can be expressed as

$$\Gamma = 2\gamma + W_p \quad (6)$$

where  $W_p$  is the work for plasticity. Unlike brittle materials, ductile materials dissipate significant energy through this plastic deformation, contributing to their higher fracture toughness.

Following in 1967, Lake and Thomas developed a model specifically for polymer networks, considering that each polymer chain is composed of numerous monomers with chemical energy stored in the C–C bonds.<sup>41</sup> In this model, fracture energy is influenced by the number of C–C bonds along stretched polymer chains. At the front of a crack, polymer chains are stretched to the point where all the C–C bonds along the chain approach their breaking threshold. The mechanical energy needed to stretch the chain to this critical state is equal to the total chemical energy stored in its C–C bonds. When the chain finally breaks, this stored mechanical energy is released



and dissipated, contributing to fracture resistance. The energy required to reach this breaking point, termed intrinsic fracture energy can be expressed as

$$\Gamma_0 = eL \quad (7)$$

where  $e$  is the chemical energy per unit volume, and  $L$  is the thickness of the single polymer chain layer in the undeformed state. The energy per unit volume can be defined as

$$e = bJ \quad (8)$$

where  $b$  is the number of single bonds per unit volume,  $J$  is the energy of a C-C bond. The single-chain layer thickness  $L$  is estimated by the end-to-end distance of the polymer chain in the undeformed state,

$$L = a\sqrt{m} \quad (9)$$

where  $a$  is the length of the monomer, and  $m$  is the number of monomers in the chain. The resulting intrinsic fracture energy can be expressed as

$$\Gamma_0 = bJa\sqrt{m} \quad (10)$$

This demonstrates that the toughness of polymer chains is proportional to the number of monomers between crosslinking points, and during crack propagation, the energy stored in the crosslinked polymer chains is dissipated once the chains break. When a polymer forms a network that incorporates energy dissipation sources, the fracture energy ( $\Gamma$ ) of the polymer can be expressed as

$$\Gamma = \Gamma_0 + \Gamma_D$$

where  $\Gamma_D$  represents dissipated fracture energy.

## 2.6 Testing methods for fracture resistance

Fracture, often an undesirable occurrence, can be assessed through various testing methods. These include tearing<sup>45</sup> or peeling tests,<sup>54</sup> where force and displacement are recorded, as well as puncture<sup>55</sup> and impact tests.<sup>56</sup> Tearing tests involve applying a tensile force to a pre-cut sample to measure the material's resistance to crack propagation. Peeling tests focus on determining the adhesive strength between two layers by measuring the force needed to peel one layer from another. Puncture tests evaluate the force required to penetrate a material using a sharp probe, simulating real-world puncture scenarios. Impact tests measure the energy absorbed when a material is subjected to sudden, high-speed loading, providing insights into its toughness under dynamic conditions. Among these, the pure shear test is widely used. For this test, two types of samples—unnotched and notched—are required.<sup>3,40</sup> Both are stretched using a UTM to obtain a force-displacement curve. For the notched sample, the critical stretch ( $\lambda_c$ ) is determined, which marks the onset of crack propagation. For the unnotched sample, the area under the force-displacement curve up to  $\lambda_c$  is integrated and divided by the cross-sectional area of the sample to determine toughness ( $\Gamma$ )<sup>45</sup> (Fig. 3d). The parameters that influence  $\Gamma$  include the strength of the unnotched sample and the resistance to crack propagation in

the notched sample. Since  $\Gamma$  is an intrinsic material property, it is valuable for comparing the fracture characteristics of different materials. However,  $\Gamma$  does not always yield consistent values due to limitations associated with measurement methods. Variations in sample dimensions can affect the measured values of  $\Gamma$ , as they influence the stress distribution within the material. Additionally, for soft materials that exhibit viscoelasticity, differences in strain rate during testing can lead to discrepancies in  $\Gamma$ , as their time-dependent behavior causes the energy dissipation to vary with the rate of deformation. To enable reliable comparisons of  $\Gamma$  across different materials, standardized testing protocols are necessary. Despite these limitations,  $\Gamma$  remains a crucial indicator for assessing whether a material is suitable for specific applications.

## 3. Enhancing elasticity or fracture resistance

### 3.1 Elastic network design

One of the most critical properties that have enabled the broad application of soft materials across various fields is undoubtedly their elasticity. Materials with high elasticity are particularly important in applications involving repeated loading and unloading or in ensuring long-term durability. Consequently, extensive research has been conducted to enhance the elasticity characteristics of soft materials composed of polymeric springs.<sup>57-59</sup> Researchers employ crosslinkers to reinforce the polymer network, leveraging entropic elasticity to enhance its elastic response. Additionally, tailoring molecular interactions within the polymer network utilizes elasticity driven by enthalpic contributions. In the following sections, we outline strategies to enhance elasticity through network topology and molecular interactions.

**3.1.1 Network topology.** In polymer networks, topology, which describes the arrangement of polymer chains and crosslinking points, is a key factor in determining mechanical properties.<sup>60</sup> Chemical crosslinkers play a significant role by controlling the network architecture.<sup>61</sup> Two principal strategies exist: increasing the density of covalent crosslinkers and adjusting their functionality.

Increasing the crosslinker density reduces the number of segments  $N$  between crosslinking points. Consequently, the number of possible conformations decreases, leading to an increased restoring force. This increased restoring force suppresses plastic deformation, facilitating the recovery to its original state, thereby enhancing elasticity.<sup>62</sup> He *et al.* demonstrated that optimizing chemical crosslinker density improved elasticity and minimized hysteresis (Fig. 4a).<sup>57</sup> This phenomenon can be explained using the standard linear solid model, which is based on Maxwell theory. Higher crosslinking density enhances the elasticity of the spring, effectively reducing creep and making the material more elastic.

Another approach involves enhancing crosslinker functionality, which refers to the number of polymer chains a single crosslinker can connect.<sup>48</sup> High-functionality crosslinkers



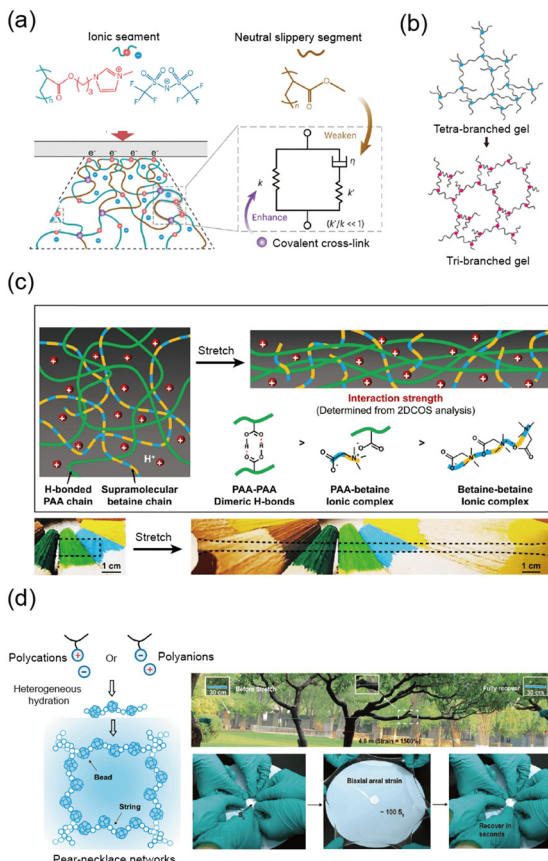


**Fig. 4** Highly elastic networks. (a) Schematic illustration of a highly cross-linked polyelectrolyte elastomers. The network enhances entropic elasticity through high crosslinking density. Reproduced with permission from ref. 57. Copyright 2024, Springer Nature. (b) Tri-branched hydrogels achieve high elasticity and stretchability through reversible strain-induced crystallization, despite their low crosslinker functionality. Reproduced with permission from ref. 63. Copyright 2022, AAAS. (c) Zwitterionic hydrogel network exhibits strain-stiffening through a dual-network design, which stiffens the network while maintaining high elasticity. Reproduced with permission from ref. 58. Copyright 2021, Springer Nature. (d) Schematic illustration of a pearl-necklace network in polyelectrolyte hydrogels. The network unfolds and refolds under mechanical strain, allowing rapid recovery and hyper elasticity. Reproduced with permission from ref. 59. Copyright 2023, AAAS.

introduce multiple polymer chains between adjacent crosslinkers, strengthening the elasticity of the network.<sup>64–66</sup> However, increasing crosslinker functionality does not always yield beneficial outcomes;<sup>63,67,68</sup> in specific polymers, such as poly(ethylene glycol) (PEG), reducing functionality can impart distinctive material properties. For example, Sakai *et al.* presented a tri-branched network structure that improved elasticity through reversible strain-induced crystallization despite its reduced functionality.<sup>63</sup> This finding highlights that lower-functionality crosslinkers can also enhance elasticity when combined with other mechanisms, such as crystallization (Fig. 4b).

Besides covalent crosslinking and their functionality, network defects such as loops and dangling ends also play a crucial role in determining elasticity.<sup>39</sup> Loops form when

polymer chains react intramolecularly instead of participating in the network structure.<sup>32</sup> This reduces the effective number of elastically active chains, leading to diminished elasticity.<sup>69</sup> By employing controlled synthesis methods to minimize loop formation, network connectivity can be improved, resulting in enhanced elasticity. Similarly, dangling ends refer to the freely moving chain ends that do not contribute to the network.<sup>70,71</sup> These defects increase the elastically inactive regions, further reducing the overall elasticity of the network. Therefore, minimizing network defects is essential for optimizing elasticity in polymer networks.

**3.1.2 Molecular interactions.** Molecular interactions are an effective mechanism for enhancing elasticity in soft materials. When interactions are properly tuned, they can break under external stress and rapidly reform, allowing the polymer conformation to revert to its original state and thus improving elasticity. These interactions, such as electrostatic interactions or metal coordination, are influenced by enthalpy changes associated with bond dissociation and reformation, which contribute to the enhancement of elasticity. The bond strength and recovery dynamics of these interactions vary across different material systems, underscoring the need to tailor molecular interactions to enhance elasticity. Achieving desired performance under repeated deformation requires a balance between interaction strength and recovery dynamics. Strategies include using electrostatic interactions,<sup>58,72–74</sup> metal coordination,<sup>75–77</sup> and hydrophilic–hydrophobic interactions.<sup>59,78–80</sup> These dynamic and reversible interactions enable the material to adapt to deformation efficiently.

Zhang *et al.* reported a skin-like ionic elastomer with a supramolecular zwitterionic network embedded within hydrogen-bonded polycarboxylic acid chains.<sup>58</sup> The two networks exhibit varying strengths, enabling sequential debonding during stretching. This unique combination of dynamic interactions enables fast recovery and high performance under cyclic stress (Fig. 4c).

Moreover, Chen *et al.* increased the elasticity of polyelectrolyte hydrogels by adjusting the water content.<sup>59</sup> With the optimal amount of water, the polymer chains form a pearl-necklace chain (PNC) structure, where (1) hydrophobic alkyl chains act as soft beads and (2) hydrophilic ionic groups form the string. Upon external deformation, the optimum amount of water acts as a lubricant, allowing reversible hydrophobic interactions to reform, further enhancing the elasticity of the material (Fig. 4d).

### 3.2 Fracture resistant network design

The elasticity of polymer networks relies on the capacity to store energy under stress and release it upon unloading. Although the ability to store and release energy is beneficial for elasticity, effective crack resistance requires energy dissipation rather than energy storage and release.<sup>81,82</sup> To make soft materials tougher, researchers have investigated strategies to improve fracture resistance by promoting energy dissipation within the polymer network.<sup>83,84</sup> A primary approach involves expanding the plastic zone, a region around a crack tip where energy



dissipation can occur more readily. In the following sections, we will explore various network design strategies that aim to increase fracture resistance by expanding the plastic zone size.

**3.2.1 Double network.** One common method for dissipating energy under mechanical stress is through the fracture of polymer chains.<sup>40,85–87</sup> To achieve efficient energy dissipation through chain fracture, the polymer chains must be designed to break in response to external deformation.

Gong *et al.* significantly increased the fracture energy of hydrogels by introducing a double network structure composed of a brittle, energy-dissipating first network and a soft, stretchable second network.<sup>46,87</sup> The fracture of the first network dissipates mechanical energy, while the second network maintains the structural integrity of the hydrogel (Fig. 5a). This method of using double networks to enhance fracture resistance has been widely studied, with many researchers focusing on the use of covalent crosslinking.<sup>43,88–93</sup>

Sun *et al.* extended this concept by creating a double network of physically crosslinked alginate and covalently cross-linked acrylamide, expanding the plastic zone to achieve even higher fracture energies of  $\sim 9000 \text{ J m}^{-2}$  (Fig. 5b).<sup>3</sup> This design introduced ionic interactions that rupture under stress, making the material more stretchable while maintaining toughness.<sup>94</sup> They further demonstrated the fracture resistance of the double network hydrogel using various multivalent cations.<sup>95</sup>

The double network design has also been applied in combination with various other networks, establishing itself as a versatile method for enhancing the mechanical properties of polymer systems.<sup>96–99</sup>

**3.2.2 Hydrogen bonds.** Hydrogen bonds represent dynamic and reversible interactions that can break and reform in response to external mechanical stress.<sup>100</sup> By adjusting the strength and distribution of hydrogen bonds, materials can exhibit a wide range of mechanical properties. Li *et al.* developed a poly(urethane-urea) hydrogel that incorporated strong hydrogen bond arrays, which significantly increased fracture energy.<sup>101</sup> Unlike the sequential fracture of polymer chains in double networks, hierarchical hydrogen bonds with varying strengths offer an alternative mechanism for enhancing fracture resistance.<sup>102–107</sup>

**3.2.3 Polyampholytes.** Ampholytes are molecules containing both acidic and basic functional groups depending on the environment.<sup>108</sup> Polyampholytes are polymers that contain both positively and negatively charged repeat units, which interact *via* electrostatic forces. Sun *et al.* synthesized polyampholyte hydrogels by random copolymerization of cationic and anionic monomers, resulting in a network with a random distribution of ionic bonds.<sup>47</sup> Strong ionic bonds function as permanent crosslinks, while weaker bonds act as sacrificial and reversible bonds. These weaker bonds dissipate mechanical energy during deformation, thereby increasing fracture resistance.<sup>47,109</sup>

**3.2.4 Metal coordination.** In polymer networks, metal ions can serve as coordination centers that interact with polymer chains or other coordinating agents, such as dipoles or ions.<sup>110</sup> The interactions between metal ions and these coordinating

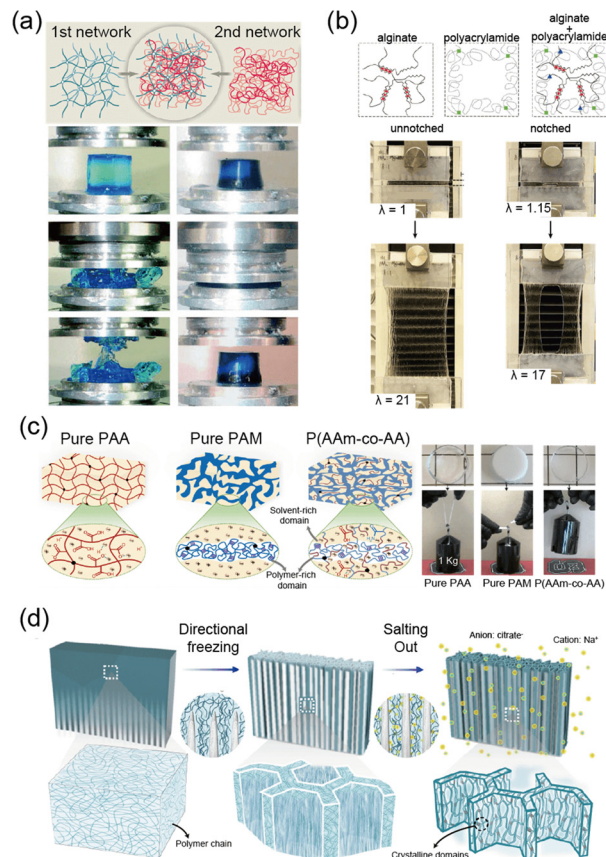


**Fig. 5** Highly tough networks. (a) Schematic illustration of a double network (DN) hydrogel composed of a rigid, brittle first network and a soft, stretchable second network. The DN hydrogel exhibits high toughness as the brittle network dissipates energy through sacrificial bond breakage. Reproduced with permission from ref. 46 and 85. Copyright 2014, AAAS, Copyright 2003, Wiley-VCH. (b) Alginate–polyacrylamide hydrogel demonstrates high stretchability and notch insensitivity due to the synergy between crack bridging by covalent crosslinks and energy dissipation through ionic crosslink unzipping. Reproduced with permission from ref. 3. Copyright 2012, Springer Nature. (c) Tough ionogel network formed through *in situ* phase separation. The polymer-rich domains enhance fracture resistance by dissipating energy, while the solvent-rich domains maintain stretchability. Reproduced with permission from ref. 20. Copyright 2022, Springer Nature. (d) Tough hydrogel formed by the synergy of freeze-casting and salting-out methods, creating a hierarchical structure with aligned nanofibrils, showing notch insensitivity when stretched. Reproduced with permission from ref. 29. Copyright 2021, Springer Nature.

entities are sufficiently strong to act as sources of energy dissipation, thereby enhancing the fracture resistance of the material.<sup>109,111–115</sup> Park *et al.* investigated the use of different ligands, including non-coordinating anions (e.g.,  $\text{OTF}^-$ ,  $\text{TFSI}^-$ ), coordinating anions (e.g.,  $\text{Cl}^-$ ), and multimodal anions (e.g.,  $\text{OAc}^-$ ,  $\text{acac}^-$ ), to measure the toughness and self-healing properties of elastomers.<sup>112</sup> Their work demonstrated the ability of metal coordination to create reversible and tough networks through metal-ligand interactions, with varying anions influencing the mechanical properties of the elastomers.

**3.2.5 Phase separation.** Phase separation within polymer networks occurs when components with differing affinities segregate, leading to the aggregation of similar components



into distinct regions.<sup>116,117</sup> Each of these regions serves a specific function, and the synergy between them contributes to enhanced mechanical properties. This combination of specialized regions enables the material to better dissipate energy, resist crack propagation, and ultimately improve fracture resistance.

Phase separation in polymer networks can manifest in two representative forms: polymer–polymer separation and polymer–solvent separation. Each method produces unique network architectures that contribute to the ability of the material to resist fracture.<sup>89,118,119</sup>

For instance, Fernández-Rico *et al.* demonstrated polymer–polymer phase separation through microphase separation within an elastomer matrix.<sup>120</sup> By supersaturating polydimethylsiloxane (PDMS) with heptafluorobutyl methacrylate (HFBMA), phase separation was induced upon cooling, forming a robust bicontinuous microstructure. This structure enhanced the fracture resistance of the material through strong interactions between similar components.

In another study, Wang *et al.* demonstrated polymer–solvent separation to create tough and stretchable ionogels through *in situ* phase separation.<sup>20</sup> The ionic liquid was miscible with poly(acrylic acid) (PAA) but immiscible with polyacrylamide (PAAm), leading to the formation of a bicontinuous polymer network. The polymer-rich domain, strengthened by hydrogen bonds, contributed to toughness, while the solvent-rich domain provided stretchability (Fig. 5c).

**3.2.6 Crystallization.** Crystalline domains within a polymer network enhance fracture resistance by acting as rigid physical crosslinks and forming hierarchical structures.<sup>30,40</sup> These structures, characterized by high chain density, require more energy to rupture than amorphous regions, thereby suppressing crack propagation. Additionally, interconnected characteristics of these crystalline domains help distribute and dissipate mechanical energy efficiently, further improving the fracture resistance of the material.<sup>121</sup>

The type of polymer and the fabrication method are key factors in achieving crystallization within polymers. Certain polymers, such as poly(vinyl alcohol) (PVA), are more prone to crystallization due to their molecular structure.<sup>122</sup> Additionally, the way the polymer is processed—through methods like annealing, freeze–thaw cycles, or salting-out—can significantly affect the degree and distribution of crystallinity within the material.

For example, Peppas *et al.* introduced crystalline domains into poly(vinyl alcohol) (PVA) hydrogels using a freeze–thaw method, which improved the ultimate tensile strength, modulus, and toughness of the hydrogels.<sup>123,124</sup> Building on this approach, Hua *et al.* combined freeze-casting and salting-out methods to create a hierarchical structure with high crystallinity in PVA hydrogels.<sup>29</sup> The crystalline regions acted as energy dissipation centers, while well-aligned nanofibrils helped blunt crack propagation (Fig. 5d).

**3.2.7 Mechano-chemistry.** Mechano-chemistry refers to the use of mechanical force to induce chemical reactions within polymer networks. When force is applied, bond scission occurs,

triggering chemical reactions that improve fracture resistance by energy dissipation of the material.<sup>125–127</sup> Wang *et al.* incorporated force-coupled chemical reactions into polymer chains, allowing the polymer strands to lengthen before breaking.<sup>128</sup> By using bicyclic cyclobutene mechanophores, the polymer network could extend by up to 40%, significantly improving fracture resistance. They further demonstrated the use of cyclobutene-based mechanophores as crosslinkers, extending their application to elastomers.<sup>129</sup>

### 3.3 General relationship between elasticity and fracture resistance

When examining network designs that enhance elasticity and fracture resistance individually, it becomes evident that the factors required to improve each property are fundamentally different. However, it is often overlooked that incorporating these factors into a single network design can negatively impact the opposing property. This trade-off becomes particularly apparent when analyzing network designs through their relationship between elasticity and fracture resistance (Fig. 6). This is because both toughness and hysteresis are generally influenced by the size of the plastic zone, which impacts these properties simultaneously. As a result, most materials fall along a predictable trend line on the Ashby plot. However, certain network designs have successfully achieved both low hysteresis and high toughness. These designs, which deviate from conventional approaches, are referred to as advanced network designs. Such designs are achieved through flawless structures, dynamically moving components during deformation, or harnessing specific molecular interactions. In the following section, we will explore network designs that simultaneously exhibit high elasticity and fracture resistance.

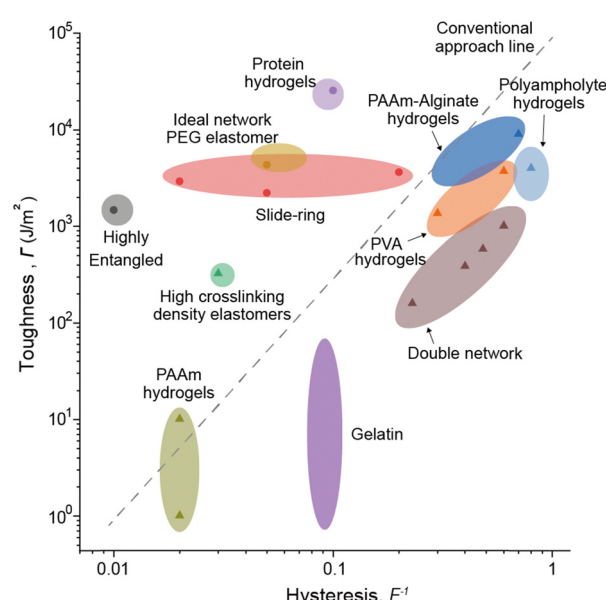


Fig. 6 Ashby plot of toughness ( $\Gamma$ ) and hysteresis based on network design. The black dashed line represents the conventional relationship between toughness and hysteresis in soft materials. Advanced network designs deviate from this conventional relationship.



## 4. Improving both elasticity and fracture resistance

Overcoming the traditional trade-off between fracture resistance and elasticity, various network designs have been developed to achieve both high toughness and low hysteresis. The approaches to resolving this trade-off relationship can be broadly categorized into three strategies: increasing elasticity without compromising fracture resistance, enhancing fracture resistance without reducing elasticity, and, finally, improving both properties simultaneously (Fig. 7). Notable examples include ideal networks, highly entangled networks, slide-ring networks, and peptide-crosslinked networks. These designs reduce hysteresis without compromising toughness by minimizing flaws in the network, enhance toughness through dynamic crosslinking, or resolve trade-offs using molecular interactions. The following sections provide an in-depth discussion of the energy dissipation and recovery mechanisms that support these network designs.

### 4.1 Flawless network design

In polymer networks, defects play a critical role in determining the mechanical performance of the material. Common defects include uneven crosslinking, unreacted chains that form dangling ends, and the formation of loops.<sup>130</sup> These irregularities act as stress concentration points under load, reducing fracture resistance. Furthermore, they hinder uniform deformation across the network, thereby lowering elasticity. To address these issues, researchers have made efforts to minimize defects and create ideal networks that make soft materials more robust.

**4.1.1 Ideal network.** An ideal network refers to a polymer network where the chains are perfectly and uniformly distributed, free from defects like loops and dangling ends.<sup>35,130-133</sup> This defect-free structure, based on network regularity, prevents stress concentration, ensuring that stress distributes evenly throughout the network. Thus, the material can stretch uniformly by dispersing the load across a greater number of chains, achieving high elasticity while maintaining fracture resistance.<sup>134-137</sup> When applied to ideal networks with long chains or chains capable of strain-induced crystallization (SIC),<sup>138-140</sup> this design can further enhance toughness and minimize hysteresis.

Kamata *et al.* developed hydrogels based on defect-free ideal networks, eliminating mechanical hysteresis without compromising fracture resistance (Fig. 8a).<sup>141</sup> The hydrogel maintains consistent mechanical properties even after multiple stretches. The synthesis involved end-linking tetra-armed PEG through step-growth polymerization. This design ensures uniform chain distribution within the hydrogel, resolving the trade-off between elasticity fracture resistance. Additionally, the isotropic extension of chains within the ideal network confers a low swellable property. This design is not limited to a single material and can be applied to a wide range of polymer networks.

The ideal network design can be applied not only to hydrogels but also to elastomers. Nakagawa *et al.* developed an elastomer with excellent mechanical properties by creating a uniform network structure with long chains (Fig. 8b).<sup>139</sup> The ideal network structure enabled uniform stress distribution across the long chains, allowing for high stretchability and toughness without sacrificing elasticity. The structure was achieved through end-linking multi-arm prepolymers, creating a highly uniform network. The uniformity facilitated chain alignment and led to strong strain-stiffening behavior. Typically, strain-stiffening is difficult to achieve due to the challenges of chain alignment after a certain level of deformation, which is often caused by defects in the network. By overcoming these limitations, this design holds potential for applications in fields such as stretchable electronics and soft robotics, where superior mechanical properties are essential.

Incorporating chains capable of SIC into an ideal network can significantly enhance the mechanical performance of elastomers.<sup>138-140</sup> SIC allows rapid recovery even after large deformations, ensuring high elasticity (Fig. 8c).<sup>138</sup> Additionally, chain alignment during deformation suppresses crack propagation. Therefore, the elastomer maintains high toughness ( $\Gamma = 5 \text{ kJ m}^{-2}$ ) and low hysteresis (<1%) even under significant strain. This design enables the material to undergo repeated deformation and recovery cycles while maintaining high performance across a broad temperature range. As the strain aligns the polymer chains, crystallization occurs, enhancing mechanical properties while also improving thermal conductivity through more efficient stress distribution. These properties make the material adaptable for applications requiring both mechanical resilience and thermal management.

The ideal network design has significant advantages for polymer network modeling, which has led to extensive theoretical studies. When a near-perfect network is achieved, it maintains fracture resistance while significantly enhancing elasticity. Moreover, applying this network design to various polymers can create synergistic effects, enhancing mechanical performance. However, from a material processing standpoint, creating such ideal networks remains challenging. Scaling up production through efficient and simplified processing methods could enable broader industrial applications and enhance their feasibility for diverse fields.

### 4.2 Dynamic cross-linked network

The mechanical properties of soft materials can vary depending on how the internal network is structured. Typically, chemically crosslinked points remain fixed under stress, whereas cross-links formed through entanglements or slide-ring mechanisms can move when stress is applied. In this section, we explore network design strategies with dynamic crosslinking that overcome trade-off between fracture resistance and elasticity. We focus on how dynamic crosslinking increases fracture resistance while maintaining elasticity.

**4.2.1 Highly entangled network.** Entanglement refers to points where polymer chains are intertwined.<sup>24</sup> These entangled points act as physical crosslinking points that can



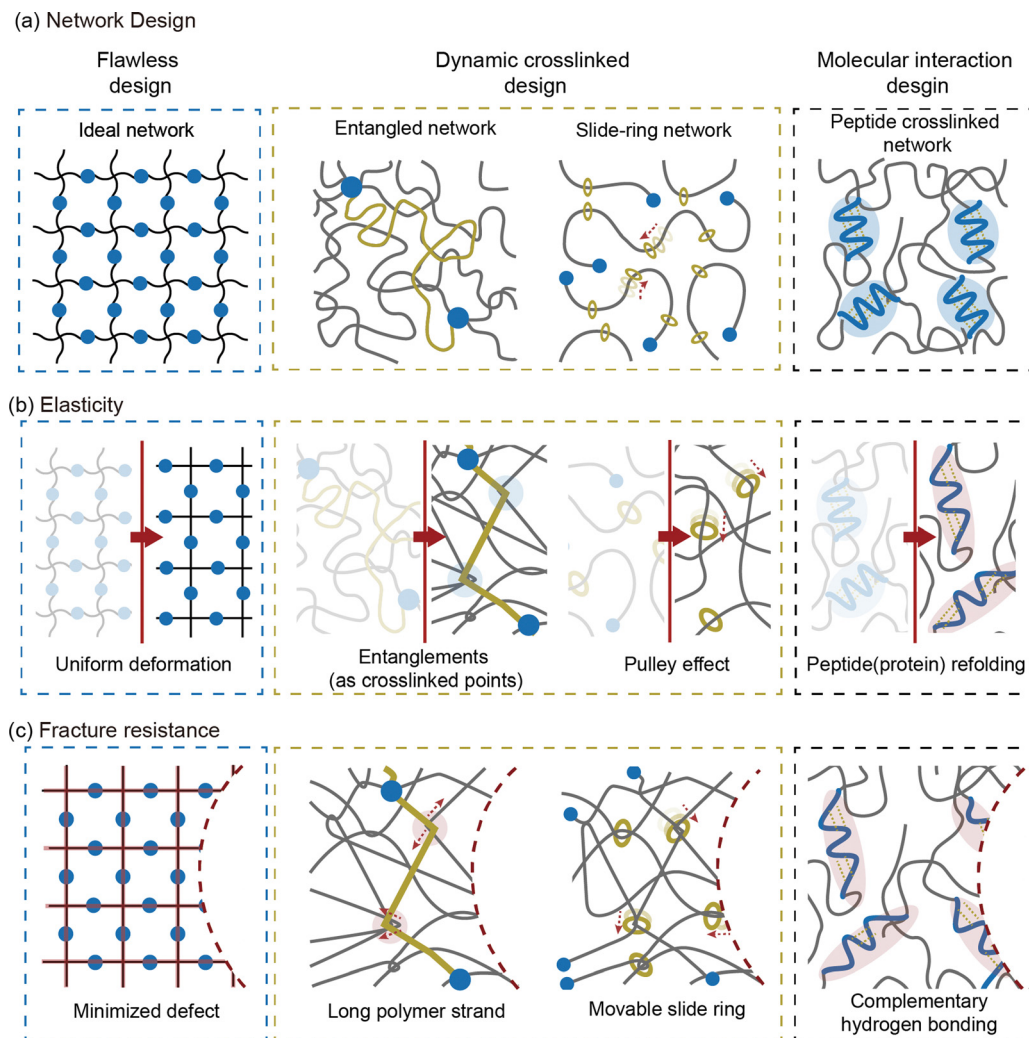


**Fig. 7** Network designs to resolve the trade-off between elasticity and fracture resistance. (a) Three main approaches exist to achieve both high toughness and low hysteresis. The flawless design minimizes defects to enhance elasticity. The dynamic crosslinked design allows crosslinking points to move, increasing fracture resistance. Lastly, the molecular interaction design, exemplified by peptide crosslinked networks, improves both elasticity and fracture resistance. (b) In terms of elasticity, each network utilizes different mechanisms: uniform deformation in ideal networks, entanglements in entangled networks, the pulley effect in slide-ring networks, and peptide (protein) refolding in peptide crosslinked networks under loading. (c) For fracture resistance, each network leverages specific structural features: minimized defects in ideal networks, long polymer strands in entangled networks, movable slide rings in slide-ring networks, and complementary hydrogen bonds in peptide (protein) crosslinked networks.

move under stress, providing flexibility similar to chemical crosslink points. This behavior enhances fracture resistance by allowing stress deconcentration through mobile crosslinks and extended chain structures.<sup>142</sup>

From eqn (10), the Lake–Thomas model suggests that the energy required to rupture a single polymer strand is directly proportional to the number of monomers in that strand ( $m$ ). As a result, increasing  $m$  can be an effective approach to improving fracture resistance. However, reducing crosslink density to increase  $m$  may enhance fracture resistance but does not lead to a decrease in elasticity. A highly entangled network design achieves high fracture toughness while maintaining elasticity (Fig. 7).<sup>38,55,97,143–153</sup>

Entanglements in polymer networks act as movable cross-links, playing a crucial role in enhancing both fracture

resistance and elasticity in soft materials. Unlike chemical crosslinkers, which are fixed within the network, polymer strands in entanglements are not confined and can move freely. This mobility enables the entanglements to act dynamically, adjusting under load by slipping and effectively increasing the length of the polymer strands experiencing stress ( $m$ ), which improves the material's ability to resist fracture. Additionally, the stress applied to one polymer strand is dispersed to others through these entanglements, reducing stress concentration across the network and further enhancing fracture resistance.

In terms of elasticity, entanglements also offer distinct characteristics. One of the key requirements for elasticity is that the internal network conformation should remain largely unchanged after the load is applied and then removed. The entangled polymer strands contribute to this by preventing



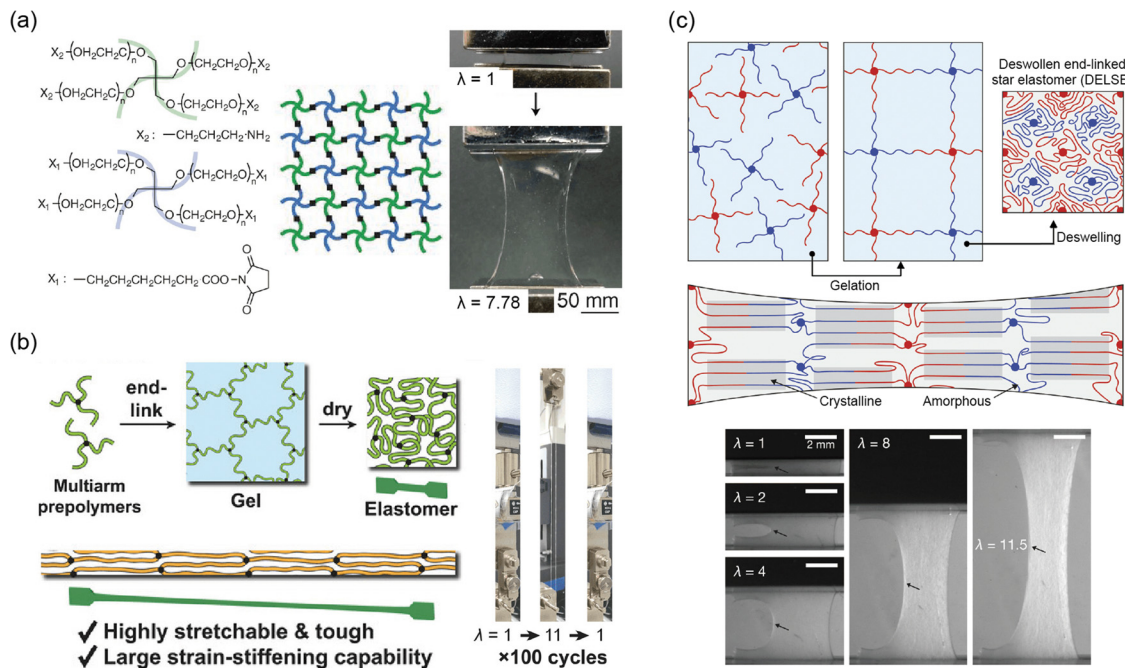


**Fig. 8** Ideal network. (a) Tetra-armed hydrogels, with a well-organized network structure, increase fracture energy without compromising elasticity, maintaining mechanical integrity under repetitive loading. Reproduced with permission from ref. 141. Copyright 2014, AAAS. (b) Elastomer with a highly homogeneous network structure demonstrates both elasticity and notch resistance due to uniform stress distribution. Reproduced with permission from ref. 139. Copyright 2023, Wiley-VCH. (c) An ideal polyethylene glycol (PEG) network with a hierarchical structure of crystalline and amorphous phases shows high toughness and elasticity, attributed to the orderly arrangement of the polymer network. Reproduced with permission from ref. 138. Copyright 2023, AAAS.

significant alterations in the network's structure under stress. Furthermore, because the network consists of long polymer chains forming these entanglements, chain rupture does not occur before material fracture, ensuring that the network returns to its original conformation after deformation. Therefore, an entanglement-based topology supports the design of materials with elasticity.

Kim *et al.* and Norioka *et al.* conducted pioneering work on synthesized soft materials where entanglements greatly outnumber crosslinks, allowing for high fracture resistance and elasticity.<sup>145,151</sup> They drastically increased the monomer concentration while adjusting the amounts of water, crosslinker, and initiator during synthesis. They show single network polyacrylamide (PAAm) hydrogels that are and have superior fracture resistance ( $\Gamma = 2 \text{ kJ m}^{-2}$ ) and elasticity ( $<1\%$ ) (Fig. 9a). This entanglements based network design is relatively simple in structure, which has led to its recent application not only in PAAm based hydrogels but also across various polymer chains. For example, Nian *et al.* developed a method to create highly elastic and tough hydrogels from doughs made of synthetic polymer chains, such as PEG.<sup>55</sup> By kneading and annealing the polymer dough, the polymer chains are densely entangled without breaking. This method is compatible with synthetic and natural polymers, opening new possibilities for sustainable, high performance hydrogels (Fig. 9b).

Recently, efforts have been made to enhance material properties by incorporating other network designs into entangled

network design. Wang *et al.* developed highly entangled double network (HEDN) hydrogels with superior mechanical properties, including high fracture resistance and elasticity.<sup>97</sup> The hydrogels use physical entanglements as effective crosslinking in the first network, leading to a highly uniform orientation under strain. This structure enables the hydrogels to achieve a high tensile strength ( $\sigma_f = 3 \text{ MPa}$ ), fracture resistance ( $\Gamma = 8 \text{ kJ m}^{-2}$ ), and strain-stiffening behavior. Unlike traditional double-network (TDN) hydrogels, which rely on energy dissipation mechanisms, HEDN hydrogels store energy in oriented polymer chains, providing high reversibility. These properties make HEDN hydrogels promising for high performance applications requiring mechanical durability (Fig. 9c).

Various approaches have been explored in the fabrication of entangled networks. Yang *et al.* introduced a simple approach by incorporating dehydration into the process.<sup>150</sup> They present a strategy for creating tough hydrogels by combining loose crosslinking with dense dehydration induced entanglements, providing a simple yet effective method for designing hydrogels that are highly resilient under stress (Fig. 9d).

In the synthesis of poly(*N*-isopropylacrylamide) (pNIPAAm) hydrogels, Cho *et al.* found that the formation of entanglements within the network varies depending on the solvent used during polymerization.<sup>38</sup> They found that *N*-isopropylacrylamide (NIPAAm) exhibits extremely high solubility in *N*-methyl formamide (NMF). Furthermore, the strong interaction between NIPAAm and NMF significantly increased the polymer's degree of polymerization, resulting in a pNIPAAm network with a high

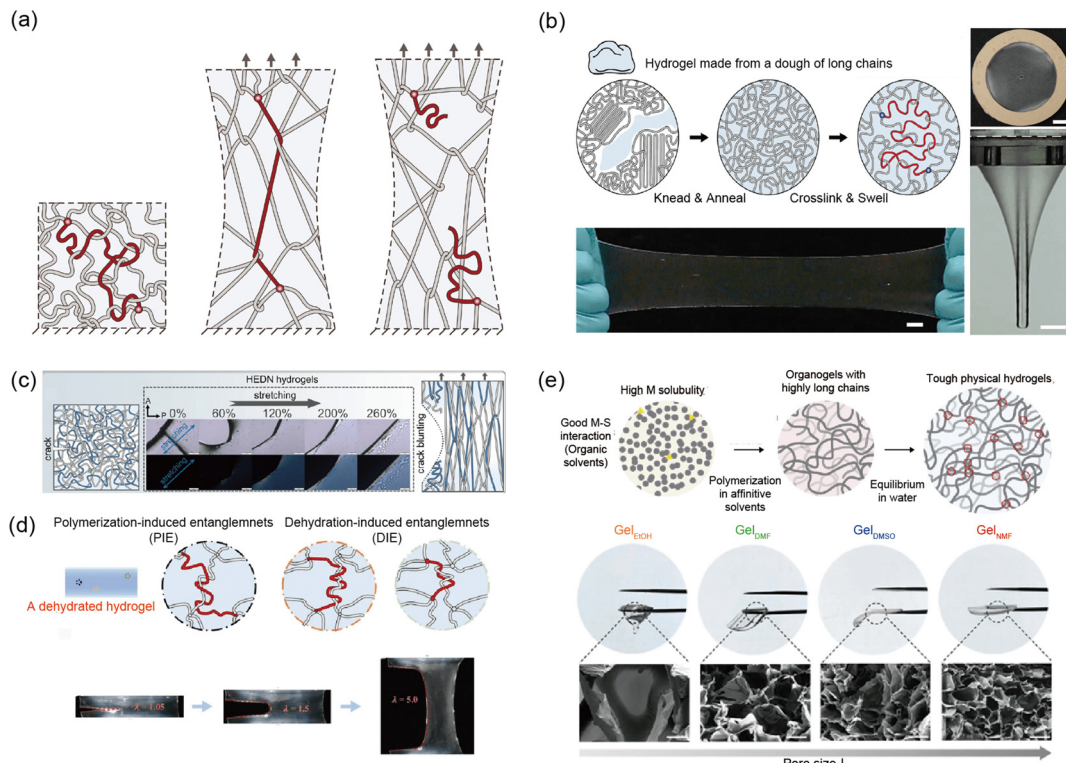


**Fig. 9** Highly entangled network. (a) Schematic illustration of a highly entangled network. The dense entanglements provide elasticity, while the long chains contribute to enhanced fracture resistance. Reproduced with permission from ref. 145. Copyright 2021, AAAS. (b) A highly entangled polyethylene glycol hydrogel demonstrates resistance to fracture when stretched or pierced with a rod. Reproduced with permission from ref. 55. Copyright 2021, Wiley-VCH. (c) The combination of a highly entangled network and a double network shows both crack blunting and enhanced elasticity when stretched. Reproduced with permission from ref. 97. Copyright 2024, Springer Nature. (d) Additional entanglements formed through dehydration in the highly entangled network enhance both elasticity and prevent crack propagation. Reproduced with permission from ref. 150. Copyright 2024, Springer Nature. (e) A tough thermo-responsive hydrogel made from highly entangled poly(N-isopropylacrylamide) (pNIPAAm) hydrogel via solvent engineering. The type of solvent affects the network formation. Reproduced with permission from ref. 38. Copyright 2024, Wiley-VCH.

degree of internal entanglement. These hydrogels, made from poly(N-isopropylacrylamide) (pNIPAAm), demonstrate significantly enhanced mechanical properties, including increased elasticity, strength, and toughness, alongside improved actuation without any additional components. The solvent engineering method improves polymer chain growth and entanglement, leading to robust thermo-responsive hydrogels (Fig. 9e).

Based on this network design, research is actively being conducted not only to enhance mechanical properties but also to explore applications of entangled network designs in various fields, such as battery electrolytes,<sup>154,155</sup> tire materials,<sup>2</sup> actuators,<sup>38</sup> and 3D printing.<sup>156</sup> However, there are limitations to the versatility of the entangled network design. Polymer entanglement is inherently influenced by the intrinsic properties of each polymer. Polymers with a low entanglement molecular weight ( $M_e$ ) for entanglement tend to form entangled networks more easily, whereas creating entangled networks with polymers of higher  $M_e$  presents challenges. Therefore, more research is needed on how to design entangled networks using polymers that are not easily entangled. Additionally, the topology of entanglements is difficult to observe directly. Since imaging entanglements is challenging, the analysis of network entanglements is still conducted indirectly through methods

such as mechanical properties, swelling ratio, and degree of polymerization. To better understand how entanglements influence the mechanical characteristics of the matrix, further research is needed to develop methods for directly analyzing entanglements.

**4.2.2 Slide-ring network.** Introducing unique structures like slide-ring (polyrotaxane) within polymer networks represents another dynamic crosslinked design approach that enhances both the fracture resistance and elasticity of soft materials. In the pioneering work by Ito *et al.* the first slide-ring was synthesized using diamino-terminated PEG with an  $\alpha$ -cyclodextrin (CD) rings.<sup>157</sup> The slide-ring network provides dynamic crosslink points as the rings act like pulleys under stress.<sup>158</sup> The pulley effect, where the polymer chain move freely through the cross links, allows the network to efficiently return to its original state after unloading. When subjected to load, the distance between two crosslinked junctions ( $m$ ) increases as the slide rings move apart. Additionally, the movement of slide rings helps disperse tension along the polymer chains, enabling efficient stress deconcentration and resulting in high fracture resistance.<sup>159–168</sup>

Slide-ring networks usually incorporate PEG, a polymer known for its crystal forming properties, and various design



approaches have utilized this feature in network development. Liu *et al.* developed a damage less reinforcement strategy for tough hydrogels using SIC.<sup>168</sup> This hydrogel structure, based on slide-ring gels, features movable crosslinks of PEG chains. Under deformation, the PEG chains align, and form crystallized structures that melt and reform, allowing for nearly 100% recovery of extension energy and providing excellent toughness. The slide-ring mechanism enables both high fracture toughness ( $3.6 \text{ kJ m}^{-2}$ ) and mechanical recoverability, making these hydrogels highly effective in applications requiring resilience under repeated stress (Fig. 10a). Hashimoto *et al.* also developed a tough slide-ring solid polymer electrolyte (SR-SPE) using SIC and phase separation mechanisms. Here, the slide-ring structure allows polymer chains to align under strain, promoting crystal formation without impairing ionic conductivity (Fig. 10b).<sup>167</sup> It is also possible to design networks by incorporating other polymers into the slide-ring network. For example, Bin Imran *et al.* developed highly stretchable thermosensitive hydrogels by incorporating slide-ring polyrotaxane (PR) crosslinkers, ionic groups, and pNIPAAm into polymer networks.<sup>159</sup> The PR crosslinkers, which enable a pulley effect, combined with ionic groups, result in hydrogels with enhanced fracture resistance and elasticity (Fig. 10c).

Recently, Yan *et al.* introduced a nanoconfined polymerization (NCP) strategy to produce tough, hysteresis free gels with remarkable crack propagation resistance and elasticity.<sup>163</sup> By confining polymerization within the nanochannels of covalent organic frameworks (COFs) or molecular sieves (MSs), this method mimics the mechanics of slide-ring structures, where

movable crosslinks allow for enhanced toughness while maintaining elasticity. This approach was successfully applied to hydrogels, ionogels, and organogels, offering a versatile strategy for material synthesis (Fig. 10d).

As numerous studies have shown, slide-ring networks exhibit superior mechanical properties in terms of fracture resistance and elasticity. These superior mechanical properties enable slide ring network to various applications, stretchable electronics,<sup>98,160,162,169,170</sup> actuators<sup>171</sup> and bioelectronics.<sup>172</sup> However, the use of polyrotaxane in constructing these networks requires specific combinations of polymers and host molecules, which inevitably limit the choices of materials for soft material fabrication. Moreover, synthesizing polyrotaxanes with low and precise host coverage is complex and challenging. Recent research has focused on developing a variety of polymers and host ring structures to construct slide-ring networks, as well as exploring approaches such as 3D printing<sup>173</sup> to facilitate the fabrication of these networks.

#### 4.3 Molecular interaction design

As discussed in Section 3, introducing specific interactions within the network can enhance fracture resistance, while incorporating reversible interactions can improve elasticity. However, the types of interactions required to enhance each mechanical property differ. Thus, achieving simultaneous improvements in both fracture resistance and elasticity through interaction-based designs presents challenges. To increase fracture resistance, strong interactions are necessary within the network to act as sources of energy dissipation. For

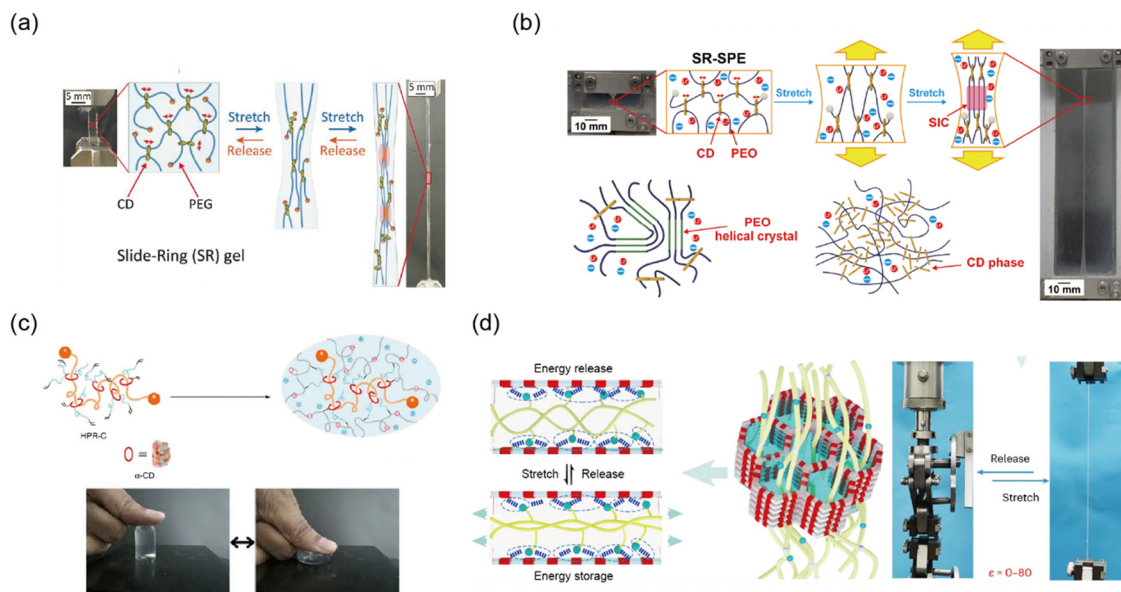


**Fig. 10** Slide-ring network. (a) An elastic and tough hydrogel was achieved by inserting polyethylene glycol (PEG) chains into hydroxypropyl- $\alpha$ -cyclodextrin (CD) rings, forming movable crosslink points. Reproduced with permission from ref. 168. Copyright 2021, AAAS. (b) The toughness of the elastic hydrogel was enhanced by adding strain-induced crystallization and phase separation to the slide-ring network. Reproduced with permission from ref. 167. Copyright 2023, AAAS. (c) The slide-ring network was applied to poly(*N*-isopropylacrylamide) (pNIPAM) hydrogels to produce a tough and elastic thermos-responsive hydrogel. Reproduced with permission from ref. 159. Copyright 2014, Springer Nature. (d) A hysteresis-free hydrogel was developed by nanoconfined polymer chains using covalent organic frameworks (COFs) or molecular sieves (MSs). The strong hydrogen bonding interactions with COFs or MSs also impart enhanced fracture resistance. Reproduced with permission from ref. 163. Copyright 2023, Springer Nature.



elasticity, precise, reversible interactions are needed to ensure that the original network conformation remains unchanged before and after load application. A type of interaction that meets both conditions is the complementary hydrogen bonding found in peptides (proteins). The refolding ability of peptides<sup>174–176</sup> after stress enhances elasticity, while complementary hydrogen bonds provide strong interactions, which thereby improve fracture resistance.

**4.3.1 Peptide (protein)-crosslinked network.** Within peptides (proteins), hydrogen bonds differ from standard hydrogen bonds. Numerous carbonyl oxygens (C=O) and amide hydrogens (NH) within the peptide backbone form complementary hydrogen bonds. These complementary hydrogen bonds enable peptides to form specific helical and coiled structures, increasing regularity. These unique structures and hydrogen bonds play a crucial role in the fracture resistance and elasticity of peptide-based networks, significantly influencing their mechanical properties. The numerous complementary hydrogen bonds within peptides can act as energy dissipation sources in the network. In coiled structures, such as helices, peptides unfold under applied load, breaking internal hydrogen bonds and allowing for energy dissipation, which increases fracture resistance. Simultaneously, the unfolded structure refolds rapidly into its original coiled form once the load is

removed, restoring the original conformation and contributing to the network's high elasticity.<sup>177–182</sup>

For example, Fu *et al.* engineered cartilage like protein hydrogels by introducing chain entanglements into folded peptides.<sup>177</sup> These hydrogels achieved a balance of high toughness and fast recovery. The design mimics the mechanical properties of cartilage, which relies on an entangled network of collagen and proteoglycans. The study demonstrated that incorporating peptide crosslinkers with chain entanglements serves as a non-covalent stiffening mechanism without compromising toughness, providing a general approach for creating stiff and tough protein-based biomaterials (Fig. 11a). Liu *et al.* developed a highly entangled polymer network strengthened by poly(L-lysine) based peptide crosslinkers.<sup>180</sup> The peptide crosslinked hydrogel exhibit excellent elasticity (<1%) and fracture resistance ( $\Gamma = 2100 \text{ J m}^{-2}$ ). The peptide based crosslinkers introduce a novel energy dissipation mechanism through the breakage of intramolecular hydrogen bonds within  $\alpha$ -helical peptide structures (Fig. 11b).

Efforts have also been made to design networks where peptides (proteins) and other polymers play distinct roles in the fracture resistance and elasticity of soft materials. Lei *et al.* developed stretchable hydrogels with low hysteresis and high anti-fatigue properties by utilizing polyprotein crosslinkers in

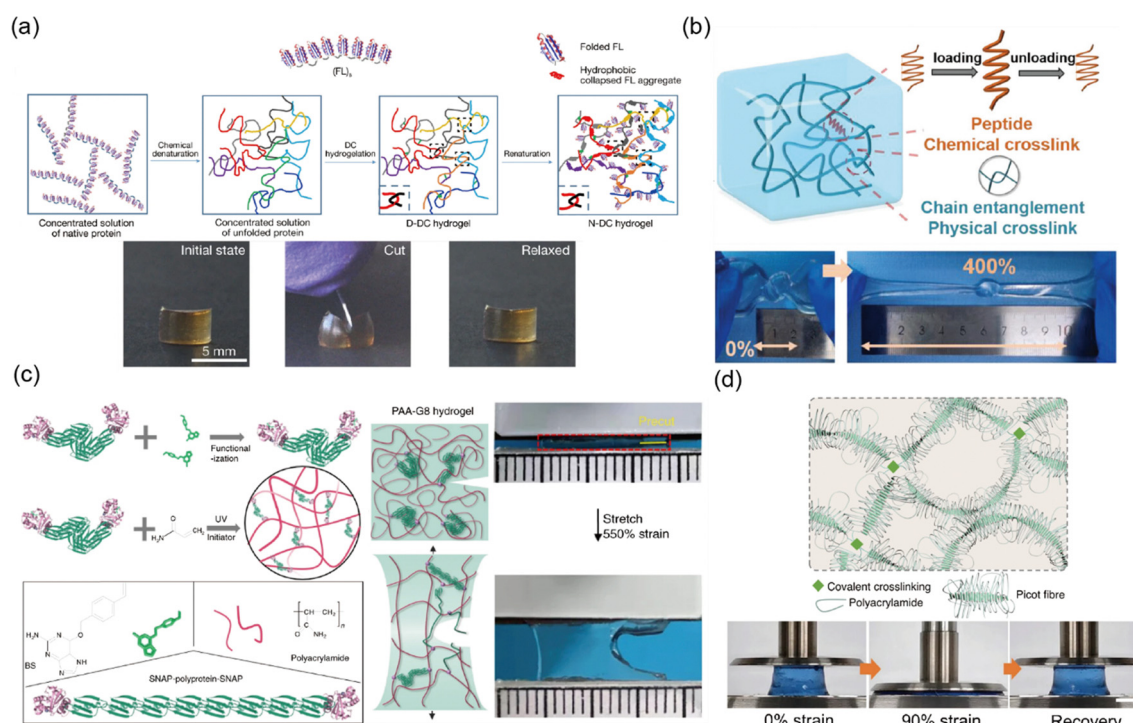


**Fig. 11** Peptide (protein) crosslinked network. (a) A cartilage-like hydrogel was created by folding proteins into a hydrophobic collapsed state within the protein hydrogel, which increased elasticity. This hydrogel is tough enough to resist cutting even when pressed with a knife. Reproduced with permission from ref. 177. Copyright 2023, Springer Nature. (b) An elastic protein-crosslinked hydrogel resists fracture, even when twisted and knotted. Reproduced with permission from ref. 180. Copyright 2023, Wiley-VCH. (c) Elastic tandem-repeat proteins were used as crosslinkers in poly(acrylic acid) (pAA) hydrogels, preventing crack propagation during stretching. Reproduced with permission from ref. 181. Copyright 2020, Springer Nature. (d) Poly(acrylamide) (pAAm) hydrogels crosslinked with picot peptide fibers exhibit rapid recovery, even after being compressed up to 90% strain. Reproduced with permission from ref. 182. Copyright 2023, Springer Nature.



combination with randomly coiled polymers.<sup>181</sup> Random coiled polymers form a percolating phase within the network, exhibiting high elasticity like highly entangled networks, while polyprotein crosslinkers unfold to prevent crack propagation. This design decouples network elasticity from local mechanical response, resulting in hydrogels with excellent elasticity ( $<5\%$ ) and high fracture resistance ( $\Gamma = 900 \text{ J m}^{-2}$ ) (Fig. 11c).

Introducing ionic coordination bonds within peptides can further enhance their energy dissipation capabilities. Xue *et al.* developed highly elastic and fatigue resistant hydrogels based on hierarchical structures of picot peptide fibers with metal coordination interaction.<sup>182</sup> These hydrogels utilize copper-bound self-assembling peptide strands with zipped flexible hidden lengths that allow for energy dissipation without reducing network connectivity. This design yields hydrogels with impressive mechanical properties, including high toughness ( $\Gamma = 25.3 \text{ kJ m}^{-2}$ ) and excellent elasticity (Fig. 11d).

Peptide crosslinker based network design gained significant research attention due to the distinct advantages of using bio-based materials, which make these networks highly applicable in biomedical fields.<sup>183</sup> For example, the high fracture resistance and elasticity of peptide-crosslinked soft materials make them suitable for cartilage replacement.<sup>177</sup> Moreover, these materials could serve as matrices for implantable devices,<sup>184</sup> such as drug delivery systems.<sup>185</sup> Therefore, the precise control of complementary hydrogen bonds in peptides opens possibilities for designing networks with a variety of tailored functions.

## 5. Conclusion and outlook

Soft materials have shown great promise for a wide range of applications. However, for practical applications, there are still significant mechanical limitations that need to be addressed. Considerable research has been conducted to improve the mechanical properties of soft materials. This review is aimed at exploring various network designs aimed at enhancing both elasticity and fracture resistance.

Traditionally, approaches used to improve fracture resistance or elasticity have struggled to achieve simultaneous improvement in both properties. Soft materials possess elasticity due to entropic elasticity, but their low energy dissipation makes them susceptible to fracture. Conversely, increasing fracture resistance by expanding the plastic zone leads to a reduction in elasticity. Recent advances in network design, including ideal networks, highly entangled networks, sliding structures, and peptide-crosslinked networks, have shown the potential to enhance both fracture resistance and elasticity.

In ideal networks, defects are minimized, allowing them to behave as nearly perfect structures. This enables uniform deformation and effective stress deconcentration, resulting in high elasticity without compromising fracture resistance. Dynamic crosslinked designs, such as slide-ring and highly entangled networks, have mobile crosslink points that respond to applied stress, dispersing the stress effectively. Slide-ring networks achieve efficient recovery through the pulley effect,

while in highly entangled networks, entanglements acting as crosslink points enhance elasticity. Lastly, peptide-crosslinked networks exhibit high elasticity and fracture resistance due to the refolding capability of peptides and complementary hydrogen bonds. These designs overcome the trade-off between fracture resistance and elasticity, achieving exceptional performance without compromise.

### 5.1 Advances in network design

Beyond the network designs discussed in this review, there is significant potential to develop new structures with superior mechanical properties. While controlling the architecture of polymers at the molecular scale has traditionally been challenging, recent advances in molecular engineering are opening new possibilities (Fig. 12, left).

Molecular engineering has enabled the on-demand control of molecular structures at the level of single molecules or oligomers.<sup>186–190</sup> Extending this level of molecular control to polymers opens the possibility of manipulating them similarly to textile fibers.<sup>191</sup> Applying textile patterns, such as weaving or knitting, to network design is expected to yield superior mechanical properties. Such designs combine the regularity of ideal networks or peptide-crosslinked networks with the mobile crosslink points found in dynamic crosslinked designs, facilitating enhanced elasticity and fracture resistance. A technology that allows polymer chains to be manipulated as freely as textile fibers would have the potential to surpass current network design capabilities.

Applying molecular engineering to soft materials enables both network formation and dynamic tuning of material properties.<sup>192,193</sup> By incorporating dynamic covalent bonds,<sup>194–197</sup> materials can now be tuned in response to stimuli. For example, soft materials utilizing DNA origami<sup>198–200</sup> and peptide-crosslinked networks, with numerous complementary hydrogen bonds, allow for precise control under external stimuli. Additionally, dynamic bonds enable recyclability and self-healing, further enhancing mechanical durability and promoting efficient resource use. Integrating these advanced molecular architectures into molecular-scale networks could unlock unprecedented mechanical properties, pushing the boundaries of soft material design.

### 5.2 Advances in fabrication strategies

Despite the promise of novel network designs, several challenges remain before soft materials can be widely applied. To be viable for practical use, these materials should be scalable for large-scale production.<sup>201</sup> Currently, soft materials are typically fabricated in laboratory settings at sizes ranging from millimeters to centimeters. Although superior mechanical properties are achievable on a small scale, scaling up to industrial production can hinder performance and introduce new manufacturing challenges. Thus, further research is needed to develop methods that ensure uniform mechanical properties at larger scales (Fig. 12, right).

Additionally, simplifying the production process for these novel networks is critical.<sup>202,203</sup> For example, ideal networks



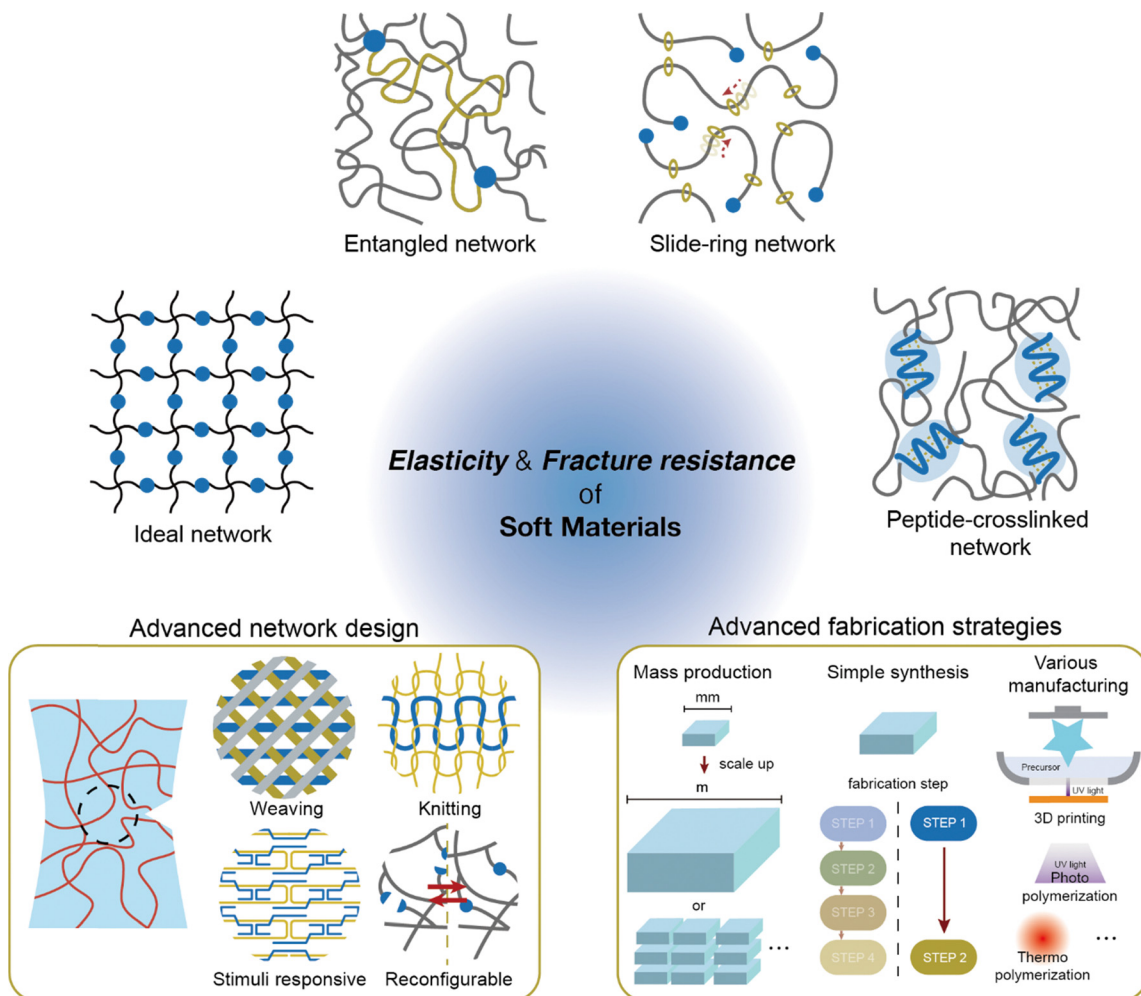


**Fig. 12** Future directions for soft material network design. This review explored network designs for both elastic and fracture-resistant soft materials (ideal networks, entangled networks, slide-ring networks, and peptide-crosslinked networks). Further research focused on developing efficient fabrication strategies (mass production, simple fabrication, and process synthesis method) for advanced network design should be addressed. The promising strategy to design next-generation novel networks based on molecular engineering (polymer weaving and knitting, stimuli-responsive and reconfigurable network).

require precisely controlled polymers to achieve a perfect structure. In particular, the synthesis of an ideal PEG network necessitates careful pH control to ensure optimal polymer formation. Similarly, the construction of highly entangled networks and slide-ring networks not only depends on the type of suitable polymers but also involves tedious processing. Highly entangled networks demand extended curing times, and constructing slide-ring networks entails additional steps to incorporate slide rings into the polymer structure. Such long or multi-step processing can limit their practical applications. Therefore, finding ways to simplify these processes is essential to advancing soft materials toward practical use.

Various manufacturing methods are also essential. Soft materials can typically be cured with light or heat, allowing for versatile shaping techniques such as molding and additive manufacturing, including 3D printing,<sup>204–206</sup> to easily create various forms. However, network designs that are both elastic and fracture-resistant often require specific conditions, which

can limit fabrication options. For instance, highly entangled networks have traditionally required long curing times, posing challenges for additive manufacturing. Recently, Dhand *et al.* demonstrated that by reducing curing time using both redox and photo-initiators, 3D printing became feasible, allowing for complex shapes and the use of multiple materials.<sup>156</sup> As new network designs are developed, processing methods that maintain their unique properties while supporting easy fabrication become essential. Ultimately, achieving simultaneous enhancement in fracture resistance and elasticity in soft materials through advanced network design and facile fabrication strategies pave the way for the next generation of soft materials.

## Author contributions

Y. E. Cho, S. Lee, and S. J. Ma contributed equally to this work. Y. E. Cho, S. Lee, and S. J. Ma conceived this work, designed



figures, and organized the outline of the manuscript. J.-Y. Sun supervised this work. All authors discussed this work and wrote the manuscript.

## Data availability

The manuscript entitled 'Network design for soft materials: addressing elasticity and fracture resistance challenges' does not include data.

## Conflicts of interest

There are no conflicts to declare.

## Acknowledgements

This work was supported by National Research Foundation of Korea (NRF) grants funded by the Korean Government (RS-2024-00459269 and RS-2021-NR059617). The Institute of Engineering Research at Seoul National University provided research facilities for this work.

## References

- 1 L. G. Treloar, *The physics of rubber elasticity*, Oxford Univ. Press, 1975.
- 2 J. Steck, J. Kim, Y. Kutsovsky and Z. Suo, *Nature*, 2023, **624**, 303–308.
- 3 J. Y. Sun, X. H. Zhao, W. R. K. Illeperuma, O. Chaudhuri, K. H. Oh, D. J. Mooney, J. J. Vlassak and Z. G. Suo, *Nature*, 2012, **489**, 133–136.
- 4 Y. S. Zhang and A. Khademhosseini, *Science*, 2017, **356**, eaaf3627.
- 5 Y.-W. Kim, J. E. Kim, Y. Jung and J.-Y. Sun, *Mater. Sci. Eng., C*, 2019, **95**, 86–94.
- 6 L. Rijns, M. G. T. A. Rutten, R. Bellan, H. Yuan, M. L. Mugnai, S. Rocha, E. del Gado, P. H. J. Kouwer and P. Y. W. Dankers, *Sci. Adv.*, 2024, **10**, eaddr3209.
- 7 J.-M. Park, J. Park, Y.-H. Kim, H. Zhou, Y. Lee, S. H. Jo, J. Ma, T.-W. Lee and J.-Y. Sun, *Nat. Commun.*, 2020, **11**, 4638.
- 8 C. Keplinger, J.-Y. Sun, C. C. Foo, P. Rothemund, G. M. Whitesides and Z. Suo, *Science*, 2013, **341**, 984–987.
- 9 C.-C. Kim, H.-H. Lee, K. H. Oh and J.-Y. Sun, *Science*, 2016, **353**, 682–687.
- 10 X. Liu, J. Liu, S. Lin and X. Zhao, *Mater. Today*, 2020, **36**, 102–124.
- 11 C. S. Park, Y.-W. Kang, H. Na and J.-Y. Sun, *Prog. Polym. Sci.*, 2024, 101791.
- 12 H. Na, Y.-W. Kang, C. S. Park, S. Jung, H.-Y. Kim and J.-Y. Sun, *Science*, 2022, **376**, 301–307.
- 13 Y. Lee, W. J. Song, Y. Jung, H. Yoo, M.-Y. Kim, H.-Y. Kim and J.-Y. Sun, *Sci. Rob.*, 2020, **5**, eaaz5405.
- 14 S.-H. Jeong, Y. Lee, M.-G. Lee, W. J. Song, J.-U. Park and J.-Y. Sun, *Nano Energy*, 2021, **79**, 105463.
- 15 S.-H. Jeong, M.-G. Lee, C.-C. Kim, J. Park, Y. Baek, B. I. Park, J. Doh and J.-Y. Sun, *Mater. Horiz.*, 2023, **10**, 2215–2225.
- 16 Y. Jiang, A. A. Trotsuk, S. Niu, D. Henn, K. Chen, C.-C. Shih, M. R. Larson, A. M. Mermin-Bunnell, S. Mittal and J.-C. Lai, *Nat. Biotechnol.*, 2023, **41**, 652–662.
- 17 R. T. Arwani, S. C. L. Tan, A. Sundarapandi, W. P. Goh, Y. Liu, F. Y. Leong, W. Yang, X. T. Zheng, Y. Yu and C. Jiang, *Nat. Mater.*, 2024, 1–8.
- 18 C. Lim, Y. J. Hong, J. Jung, Y. Shin, S.-H. Sunwoo, S. Baik, O. K. Park, S. H. Choi, T. Hyeon and J. H. Kim, *Sci. Adv.*, 2021, **7**, eabd3716.
- 19 M. Wang, X. Xiao, S. Siddika, M. Shamsi, E. Frey, W. Qian, W. Bai, B. T. O'Connor and M. D. Dickey, *Nature*, 2024, 1–6.
- 20 M. X. Wang, P. Y. Zhang, M. Shamsi, J. L. Thelen, W. Qian, V. K. Truong, J. Ma, J. Hu and M. D. Dickey, *Nat. Mater.*, 2022, **21**, 359–365.
- 21 J.-Y. Sun, C. Keplinger, G. M. Whitesides and Z. Suo, *Adv. Mater.*, 2014, **26**, 7608–7614.
- 22 J. Li, Z. Suo and J. J. Vlassak, *J. Mater. Chem. B*, 2014, **2**, 6708–6713.
- 23 P. J. Flory, *Polym. J.*, 1985, **17**, 1–12.
- 24 S. Edwards and T. Vilgis, *Polymer*, 1986, **27**, 483–492.
- 25 S. K. Goswami, C. J. McAdam, L. R. Hanton and S. C. Moratti, *Macromol. Rapid Commun.*, 2017, **38**, 1700103.
- 26 W. Wu, J. Fan, C. Zeng, X. Cheng, X. Liu, S. Guo, R. Sun, L. Ren, Z. Hao and X. Zeng, *Adv. Mater.*, 2024, **36**, 2403661.
- 27 J. Ju, G. E. Sanoja, L. Cipelletti, M. Ciccotti, B. Zhu, T. Narita, C. Yuen Hui and C. Creton, *Proc. Natl. Acad. Sci. U. S. A.*, 2024, **121**, e2410515121.
- 28 S. T. Lin, C. D. Londono, D. C. Zheng and X. H. Zhao, *Soft Matter*, 2022, **18**, 5742–5749.
- 29 M. Hua, S. Wu, Y. Ma, Y. Zhao, Z. Chen, I. Frenkel, J. Strzalka, H. Zhou, X. Zhu and X. He, *Nature*, 2021, **590**, 594–599.
- 30 X. Li and J. P. Gong, *Nat. Rev. Mater.*, 2024, 1–19.
- 31 A. V. Dobrynin and J. M. Y. Carrillo, *Macromolecules*, 2011, **44**, 140–146.
- 32 M. J. Zhong, R. Wang, K. Kawamoto, B. D. Olsen and J. A. Johnson, *Science*, 2016, **353**, 1264–1268.
- 33 M. Vatankhah-Varnosfaderani, W. F. M. Daniel, M. H. Everhart, A. A. Pandya, H. Y. Liang, K. Matyjaszewski, A. V. Dobrynin and S. S. Sheiko, *Nature*, 2017, **549**, 497–501.
- 34 A. V. Dobrynin, Y. Tian, M. Jacobs, E. A. Nikitina, D. A. Ivanov, M. Maw, F. Vashahi and S. S. Sheiko, *Nat. Mater.*, 2023, **22**, 1394–1400.
- 35 K. Urayama, *Polym. J.*, 2008, **40**, 669–678.
- 36 B. Deng, S. Wang, C. Hartquist and X. Zhao, *Phys. Rev. Lett.*, 2023, **131**, 228102.
- 37 S. P. O. Danielsen, H. K. Beech, S. Wang, B. M. El-Zaatari, X. D. Wang, L. Sapir, T. Ouchi, Z. Wang, P. N. Johnson, Y. X. Hu, D. J. Lundberg, G. Stoychev, S. L. Craig, J. A. Johnson, J. A. Kalow, B. D. Olsen and M. Rubinstein, *Chem. Rev.*, 2021, **121**, 5042–5092.

38 Y. E. Cho, J. M. Park, W. J. Song, M. G. Lee and J. Y. Sun, *Adv. Mater.*, 2024, **36**, e2406103.

39 Y. W. Gu, J. L. Zhao and J. A. Johnson, *Angew. Chem., Int. Ed.*, 2020, **59**, 5022–5049.

40 X. Zhao, *Soft Matter*, 2014, **10**, 672–687.

41 G. J. Lake and A. G. Thomas, *Proc. R. Soc. London, Ser. A*, 1967, **300**, 108–119.

42 B. Hopkinson and T. G. Williams, *Proc. R. Soc. London, Ser. A*, 1912, **87**, 502–511.

43 Y. Tanaka, R. Kuwabara, Y.-H. Na, T. Kurokawa, J. P. Gong and Y. Osada, *J. Phys. Chem. B*, 2005, **109**, 11559–11562.

44 R. Bai, J. Yang and Z. Suo, *Eur. J. Mech. A*, 2019, **74**, 337–370.

45 R. Long and C.-Y. Hui, *Soft Matter*, 2016, **12**, 8069–8086.

46 J. P. Gong, Y. Katsuyama, T. Kurokawa and Y. Osada, *Adv. Mater.*, 2003, **15**, 1155–1158.

47 T. L. Sun, T. Kurokawa, S. Kuroda, A. B. Ihsan, T. Akasaki, K. Sato, M. A. Haque, T. Nakajima and J. P. Gong, *Nat. Mater.*, 2013, **12**, 932–937.

48 P. J. Flory, *Principles of polymer chemistry*, Cornell University Press, 1953.

49 P. J. Flory and M. Volkenstein, *Biopolymers*, 1969, **8**, 699–700.

50 L. Gao, B.-L. Hu, L. Wang, J. Cao, R. He, F. Zhang, Z. Wang, W. Xue, H. Yang and R.-W. Li, *Science*, 2023, **381**, 540–544.

51 A. Griffith, *Trans. R. Soc. London, Ser. A*, 1920, **221**, 163–198.

52 G. R. Irwin, *Fracturing of metals*, 1947.

53 E. Orowan, *Rep. Prog. Phys.*, 1949, **12**, 185.

54 Y. Wang, T. Yin and Z. Suo, *J. Mech. Phys. Solids*, 2021, **150**, 104348.

55 G. Nian, J. Kim, X. Bao and Z. Suo, *Adv. Mater.*, 2022, **34**, e2206577.

56 J. Zhang, Y. Miao, Q. Qin, T. Lu, Y. Ye, H. He, J. Wang and H. Li, *Mech. Mater.*, 2021, **154**, 103717.

57 Y. He, Y. Cheng, C. Yang and C. F. Guo, *Nat. Mater.*, 2024, 1–8.

58 W. Zhang, B. Wu, S. Sun and P. Wu, *Nat. Commun.*, 2021, **12**, 4082.

59 L. Chen, Z. Jin, W. Feng, L. Sun, H. Xu and C. Wang, *Science*, 2024, **383**, 1455–1461.

60 P. J. Flory, *Br. Polym. J.*, 1985, **17**, 96–102.

61 Y. Gu, J. Zhao and J. A. Johnson, *Trends Chem.*, 2019, **1**, 318–334.

62 M. Rubinstein and R. H. Colby, *Polymer Physics*, Oxford University Press, 2003.

63 T. Fujiyabu, N. Sakumichi, T. Katashima, C. Liu, K. Mayumi, U.-I. Chung and T. Sakai, *Sci. Adv.*, 2022, **8**, eabk0010.

64 Y. Masubuchi, *Polym. J.*, 2024, **56**, 163–171.

65 C. Zhou and Q. Wu, *Colloids Surf., B*, 2011, **84**, 155–162.

66 K. Hashimoto, T. Enoki, C. Liu, X. Li, T. Sakai and K. Mayumi, *Macromolecules*, 2024, **57**, 1461–1468.

67 H. Shi, W. Zhou, Z. Wen, W. Wang, X. Zeng, R. Sun and L. Ren, *Mater. Horiz.*, 2023, **10**, 928–937.

68 M. E. Seitz, D. Martina, T. Baumberger, V. R. Krishnan, C.-Y. Hui and K. R. Shull, *Soft Matter*, 2009, **5**, 447–456.

69 Y. Gu, K. Kawamoto, M. Zhong, M. Chen, M. J. Hore, A. M. Jordan, L. T. Korley, B. D. Olsen and J. A. Johnson, *Proc. Natl. Acad. Sci. U. S. A.*, 2017, **114**, 4875–4880.

70 C. Tsengoglou, *Macromolecules*, 1989, **22**, 284–289.

71 A. k Zhang, J. Ling, K. Li, G. d Fu, T. Nakajima, T. Nonoyama, T. Kurokawa and J. P. Gong, *J. Polym. Sci., Part B: Polym. Phys.*, 2016, **54**, 1227–1236.

72 S. Guan, C. Xu, X. Dong and M. Qi, *J. Mater. Chem. A*, 2023, **11**, 15404–15415.

73 Z. Zhang, L. Qian, J. Cheng, C. Ma and G. Zhang, *Adv. Funct. Mater.*, 2024, 2402115.

74 X. Yu, Y. Wang, H. Zhang, Z. Li, Y. Zheng, X. Fan, Y. Lv, X. Zhang and T. Liu, *Chem. Mater.*, 2023, **35**, 9287–9298.

75 J. Wang, F. Tang, C. Yao and L. Li, *Adv. Funct. Mater.*, 2023, **33**, 2214935.

76 W. Sun, B. Xue, Q. Fan, R. Tao, C. Wang, X. Wang, Y. Li, M. Qin, W. Wang and B. Chen, *Sci. Adv.*, 2020, **6**, eaaz9531.

77 G. Zhang, S. Chen, Z. Peng, W. Shi, Z. Liu, H. Shi, K. Luo, G. Wei, H. Mo and B. Li, *ACS Appl. Mater. Interfaces*, 2021, **13**, 12531–12540.

78 T. Li, X. Li, J. Yang, H. Sun and J. Sun, *Adv. Mater.*, 2023, **35**, 2307990.

79 X. Yu, Z. Wang, Z. Li, X. Fan and T. Liu, *Chem. Mater.*, 2024, **36**, 9822–9833.

80 K. Xu, K. Shen, J. Yu, Y. Yang, Y. Wei, P. Lin, Q. Zhang, C. Xiao, Y. Zhang and Y. Cheng, *Chem. Mater.*, 2022, **34**, 3311–3322.

81 X. Guo, Y. Dong, J. Qin, Q. Zhang, H. Zhu and S. Zhu, *Adv. Mater.*, 2024, 2312816.

82 C. Yang and Z. Suo, *Nat. Rev. Mater.*, 2018, **3**, 125–142.

83 E. Zhang, R. Bai, X. P. Morelle and Z. Suo, *Soft Matter*, 2018, **14**, 3563–3571.

84 T. Baumberger, C. Caroli and D. Martina, *Nat. Mater.*, 2006, **5**, 552–555.

85 J. P. Gong, *Science*, 2014, **344**, 161–162.

86 T. Nakajima, H. Furukawa, Y. Tanaka, T. Kurokawa, Y. Osada and J. P. Gong, *Macromolecules*, 2009, **42**, 2184–2189.

87 J. P. Gong, *Soft Matter*, 2010, **6**, 2583–2590.

88 J. Yang, K. Li, C. Tang, Z. Liu, J. Fan, G. Qin, W. Cui, L. Zhu and Q. Chen, *Adv. Funct. Mater.*, 2022, **32**, 2110244.

89 Y. Zheng, R. Kiyama, T. Matsuda, K. Cui, X. Li, W. Cui, Y. Guo, T. Nakajima, T. Kurokawa and J. P. Gong, *Chem. Mater.*, 2021, **33**, 3321–3334.

90 Q. Chen, L. Zhu, C. Zhao, Q. Wang and J. Zheng, *Adv. Mater.*, 2013, **25**, 4171–4176.

91 S. Naficy, J. M. Razal, P. G. Whitten, G. G. Wallace and G. M. Spinks, *J. Polym. Sci., Part B: Polym. Phys.*, 2012, **50**, 423–430.

92 T. Matsuda, T. Nakajima and J. P. Gong, *Chem. Mater.*, 2019, **31**, 3766–3776.

93 J. Murai, T. Nakajima, T. Matsuda, K. Tsunoda, T. Nonoyama, T. Kurokawa and J. P. Gong, *Polymer*, 2019, **178**, 121686.

94 C. Jiang, Y. Mai, W. Li and B. Liao, *Macromol. Chem. Phys.*, 2020, **221**, 1900516.



95 C. H. Yang, M. X. Wang, H. Haider, J. H. Yang, J.-Y. Sun, Y. M. Chen, J. Zhou and Z. Suo, *ACS Appl. Mater. Interfaces*, 2013, **5**, 10418–10422.

96 K. Chen, Y. Feng, Y. Zhang, L. Yu, X. Hao, F. Shao, Z. Dou, C. An, Z. Zhuang and Y. Luo, *ACS Appl. Mater. Interfaces*, 2019, **11**, 36458–36468.

97 R. Zhu, D. Zhu, Z. Zheng and X. Wang, *Nat. Commun.*, 2024, **15**, 1344.

98 S. Wang, Y. Chen, Y. Sun, Y. Qin, H. Zhang, X. Yu and Y. Liu, *Commun. Mater.*, 2022, **3**, 2.

99 Z. J. Wang, J. Jiang, Q. Mu, S. Maeda, T. Nakajima and J. P. Gong, *J. Am. Chem. Soc.*, 2022, **144**, 3154–3161.

100 Y. Ren and X. Dong, *Prog. Polym. Sci.*, 2024, 101890.

101 Z. Li, Y. L. Zhu, W. Niu, X. Yang, Z. Jiang, Z. Y. Lu, X. Liu and J. Sun, *Adv. Mater.*, 2021, **33**, 2101498.

102 H. J. Zhang, L. Wang, X. Wang, Q. Han and X. You, *Soft Matter*, 2020, **16**, 4723–4727.

103 L. Chen, W. You, J. Wang, X. Yang, D. Xiao, H. Zhu, Y. Zhang, G. Li, W. Yu and J. L. Sessler, *J. Am. Chem. Soc.*, 2023, **146**, 1109–1121.

104 H. Zhang, W. Niu and S. Zhang, *ACS Appl. Mater. Interfaces*, 2018, **10**, 32640–32648.

105 J. Wu, F. Zeng, Z. Fan, S. Xuan, Z. Hua and G. Liu, *Adv. Funct. Mater.*, 2024, 2410518.

106 J. Chen, Y. Gao, L. Shi, W. Yu, Z. Sun, Y. Zhou, S. Liu, H. Mao, D. Zhang and T. Lu, *Nat. Commun.*, 2022, **13**, 4868.

107 H. Fan, J. Wang and Z. Jin, *Macromolecules*, 2018, **51**, 1696–1705.

108 J.-M. Park, S. Lim and J.-Y. Sun, *Soft Matter*, 2022, **18**, 6487–6510.

109 Y. Huang, L. Xiao, J. Zhou, T. Liu, Y. Yan, S. Long and X. Li, *Adv. Funct. Mater.*, 2021, **31**, 2103917.

110 G. A. Lawrance, *Introduction to coordination chemistry*, John Wiley & Sons, 2013.

111 C.-H. Li, C. Wang, C. Keplinger, J.-L. Zuo, L. Jin, Y. Sun, P. Zheng, Y. Cao, F. Lissel and C. Linder, *Nat. Chem.*, 2016, **8**, 618–624.

112 H. Park, T. Kang, H. Kim, J.-C. Kim, Z. Bao and J. Kang, *Nat. Commun.*, 2023, **14**, 5026.

113 S. C. Grindy, R. Learsch, D. Mozhdehi, J. Cheng, D. G. Barrett, Z. Guan, P. B. Messersmith and N. Holten-Andersen, *Nat. Mater.*, 2015, **14**, 1210–1216.

114 J.-C. Lai, X.-Y. Jia, D.-P. Wang, Y.-B. Deng, P. Zheng, C.-H. Li, J.-L. Zuo and Z. Bao, *Nat. Commun.*, 2019, **10**, 1164.

115 W. Li, L. Li, Z. Liu, S. Zheng, Q. Li and F. Yan, *Adv. Mater.*, 2023, **35**, 2301383.

116 S. Krause, *J. Macromol. Sci., Rev. Polym. Technol.*, 1972, **7**, 251–314.

117 M. Shaw, *J. Appl. Polym. Sci.*, 1974, **18**, 449–472.

118 F. Zhu, S. Feng, Z. Wang, Z. Zuo, S. Zhu, W. Yu, Y. N. Ye, M. An, J. Qian and Z. L. Wu, *Macromolecules*, 2023, **56**, 5881–5890.

119 L. Wang, L. Guo, K. Zhang, Y. Xia, J. Hao and X. Wang, *Angew. Chem., Int. Ed.*, 2023, **62**, e202301762.

120 C. Fernández-Rico, S. Schreiber, H. Oudich, C. Lorenz, A. Sicher, T. Sai, V. Bauernfeind, S. Heyden, P. Carrara and L. D. Lorenzis, *Nat. Mater.*, 2024, **23**, 124–130.

121 X. Liang, G. Chen, S. Lin, J. Zhang, L. Wang, P. Zhang, Z. Wang, Z. Wang, Y. Lan and Q. Ge, *Adv. Mater.*, 2021, **33**, 2102011.

122 M. Wang, J. Bai, K. Shao, W. Tang, X. Zhao, D. Lin, S. Huang, C. Chen, Z. Ding and J. Ye, *Int. J. Polym. Sci.*, 2021, **2021**, 2225426.

123 N. A. Peppas and E. W. Merrill, *J. Polym. Sci., Polym. Chem. Ed.*, 1976, **14**, 441–457.

124 N. A. Peppas and E. W. Merrill, *J. Biomed. Mater. Res.*, 1977, **11**, 423–434.

125 S. Lin, J. Liu, X. Liu and X. Zhao, *Proc. Natl. Acad. Sci. U. S. A.*, 2019, **116**, 10244–10249.

126 G. Wei, Y. Kudo, T. Matsuda, Z. J. Wang, Q. F. Mu, D. R. King, T. Nakajima and J. P. Gong, *Mater. Horiz.*, 2023, **10**, 4882–4891.

127 M. Du, H. A. Houck, Q. Yin, Y. Xu, Y. Huang, Y. Lan, L. Yang, F. E. Du Prez and G. Chang, *Nat. Commun.*, 2022, **13**, 3231.

128 Z. Wang, X. Zheng, T. Ouchi, T. B. Kouznetsova, H. K. Beech, S. Av-Ron, T. Matsuda, B. H. Bowser, S. Wang and J. A. Johnson, *Science*, 2021, **374**, 193–196.

129 S. Wang, Y. Hu, T. B. Kouznetsova, L. Sapir, D. Chen, A. Herzog-Arbeitman, J. A. Johnson, M. Rubinstein and S. L. Craig, *Science*, 2023, **380**, 1248–1252.

130 C. Yang, T. Yin and Z. Suo, *J. Mech. Phys. Solids*, 2019, **131**, 43–55.

131 Y. Akagi, T. Matsunaga, M. Shibayama, U.-I. Chung and T. Sakai, *Macromolecules*, 2010, **43**, 488–493.

132 T. Sakai, *Polym. J.*, 2014, **46**, 517–523.

133 T. Matsunaga, T. Sakai, Y. Akagi, U.-I. Chung and M. Shibayama, *Macromolecules*, 2009, **42**, 1344–1351.

134 K. Fujii, H. Asai, T. Ueki, T. Sakai, S. Imaizumi, U.-I. Chung, M. Watanabe and M. Shibayama, *Soft Matter*, 2012, **8**, 1756–1759.

135 T. Sakai, Y. Akagi, T. Matsunaga, M. Kurakazu, U. I. Chung and M. Shibayama, *Macromol. Rapid Commun.*, 2010, **31**, 1954–1959.

136 X. Li, S. Nakagawa, Y. Tsuji, N. Watanabe and M. Shibayama, *Sci. Adv.*, 2019, **5**, eaax8647.

137 Y. J. Liu, L. H. Fu, S. Liu, L. Y. Meng, Y. Y. Li and M. G. Ma, *J. Mater. Chem. B*, 2016, **4**, 4847–4854.

138 C. M. Hartquist, S. Lin, J. H. Zhang, S. Wang, M. Rubinstein and X. Zhao, *Sci. Adv.*, 2023, **9**, eadj0411.

139 S. Nakagawa, D. Aoki, Y. Asano and N. Yoshie, *Adv. Mater.*, 2023, **35**, e2301124.

140 C. M. Hartquist, B. X. Li, J. H. Zhang, Z. H. Yu, G. X. Lv, J. Shin, S. V. Boriskina, G. Chen, X. H. Zhao and S. T. Lin, *Nat. Commun.*, 2024, **15**, 5590.

141 H. Kamata, Y. Akagi, Y. Kayasuga-Kariya, U. I. Chung and T. Sakai, *Science*, 2014, **343**, 873–875.

142 S. Schlögl, M.-L. Trutschel, W. Chassé, G. Riess and K. Saalwächter, *Macromolecules*, 2014, **47**, 2759–2773.

143 D. Li, W. Zhan, W. Zuo, L. Li, J. Zhang, G. Cai and Y. Tian, *Chem. Eng. J.*, 2022, **450**, 138417.

144 Y. Feng, S. Wang, Y. Li, W. Ma, G. Zhang, M. Yang, H. Li, Y. Yang and Y. Long, *Adv. Funct. Mater.*, 2023, **33**, 2211027.

145 J. Kim, G. Zhang, M. Shi and Z. Suo, *Science*, 2021, **374**, 212–216.

146 Y. Li, X. Feng, C. Sui, J. Xu, W. Zhao and S. Yan, *Chem. Eng. J.*, 2024, **479**, 147689.

147 M. Shi, J. Kim, G. Nian and Z. Suo, *Extreme Mech. Lett.*, 2023, **59**, 101953.

148 P. Hu, J. Madsen and A. L. Skov, *Nat. Commun.*, 2022, **13**, 370.

149 P. Zhou, W. Zhan, S. Shen, H. Zhang, Z. Zou and X. Lyu, *Adv. Funct. Mater.*, 2024, 2402952.

150 D. Zhong, Z. Wang, J. Xu, J. Liu, R. Xiao, S. Qu and W. Yang, *Nat. Commun.*, 2024, **15**, 5896.

151 C. Norioka, Y. Inamoto, C. Hajime, A. Kawamura and T. Miyata, *NPG Asia Mater.*, 2021, **13**, 34.

152 Y. Kamiyama, R. Tamate, T. Hiroi, S. Samitsu, K. Fujii and T. Ueki, *Sci. Adv.*, 2022, **8**, eadd0226.

153 A. Saruwatari, Y. Kamiyama, A. Kawamura, T. Miyata, R. Tamate and T. Ueki, *Soft Matter*, 2024, **20**, 7566–7572.

154 Q. He, Z. Chang, Y. Zhong, S. Chai, C. Fu, S. Liang, G. Fang and A. Pan, *ACS Energy Lett.*, 2023, **8**, 5253–5263.

155 Z. Shen, Y. Liu, Z. Li, Z. Tang, J. Pu, L. Luo, Y. Ji, J. Xie, Z. Shu and Y. Yao, *Adv. Funct. Mater.*, 2024, 2406620.

156 A. P. Dhand, M. D. Davidson, H. M. Zlotnick, T. J. Kolibaba, J. P. Killgore and J. A. Burdick, *Science*, 2024, **385**, 566–572.

157 Y. Okumura and K. Ito, *Adv. Mater.*, 2001, **13**, 485–487.

158 T. Karino, Y. Okumura, C. Zhao, T. Kataoka, K. Ito and M. Shibayama, *Macromolecules*, 2005, **38**, 6161–6167.

159 A. Bin Imran, K. Esaki, H. Gotoh, T. Seki, K. Ito, Y. Sakai and Y. Takeoka, *Nat. Commun.*, 2014, **5**, 5124.

160 L. Feng, S. S. Jia, Y. Chen and Y. Liu, *Chem. – Eur. J.*, 2020, **26**, 14080–14084.

161 L. Jiang, C. Liu, K. Mayumi, K. Kato, H. Yokoyama and K. Ito, *Chem. Mater.*, 2018, **30**, 5013–5019.

162 R. Du, T. Bao, T. Zhu, J. Zhang, X. Huang, Q. Jin, M. Xin, L. Pan, Q. Zhang and X. Jia, *Adv. Funct. Mater.*, 2023, **33**, 2212888.

163 W. Li, X. Wang, Z. Liu, X. Zou, Z. Shen, D. Liu, L. Li, Y. Guo and F. Yan, *Nat. Mater.*, 2024, **23**, 131–138.

164 H. Gotoh, C. Liu, A. B. Imran, M. Hara, T. Seki, K. Mayumi, K. Ito and Y. Takeoka, *Sci. Adv.*, 2018, **4**, eaat7629.

165 Z. Xu, J. Lu, D. Lu, Y. Li, H. Lei, B. Chen, W. Li, B. Xue, Y. Cao and W. Wang, *Nat. Commun.*, 2024, **15**, 4895.

166 S. Y. Zheng, C. Liu, L. Jiang, J. Lin, J. Qian, K. Mayumi, Z. L. Wu, K. Ito and Q. Zheng, *Macromolecules*, 2019, **52**, 6748–6755.

167 K. Hashimoto, T. Shiwaku, H. Aoki, H. Yokoyama, K. Mayumi and K. Ito, *Sci. Adv.*, 2023, **9**, eadi8505.

168 C. Liu, N. Morimoto, L. Jiang, S. Kawahara, T. Noritomi, H. Yokoyama, K. Mayumi and K. Ito, *Science*, 2021, **372**, 1078–1081.

169 Z. Zhang, W. Wang, Y. Jiang, Y.-X. Wang, Y. Wu, J.-C. Lai, S. Niu, C. Xu, C.-C. Shih and C. Wang, *Nature*, 2022, **603**, 624–630.

170 Y. Bai, W. Li, Y. Tie, Y. Kou, Y. X. Wang and W. Hu, *Adv. Mater.*, 2023, **35**, 2303245.

171 D. Yang, F. Ge, M. Tian, N. Ning, L. Zhang, C. Zhao, K. Ito, T. Nishi, H. Wang and Y. Luan, *J. Mater. Chem. A*, 2015, **3**, 9468–9479.

172 Y. Jiang, Z. Zhang, Y.-X. Wang, D. Li, C.-T. Coen, E. Hwaun, G. Chen, H.-C. Wu, D. Zhong and S. Niu, *Science*, 2022, **375**, 1411–1417.

173 M. Tang, D. Zheng, J. Samanta, E. H. Tsai, H. Qiu, J. A. Read and C. Ke, *Chem.*, 2023, **9**, 3515–3531.

174 J. M. Fernandez and H. Li, *Science*, 2004, **303**, 1674–1678.

175 Y. Cao, T. Yoo, S. Zhuang and H. Li, *J. Mol. Biol.*, 2008, **378**, 1132–1141.

176 J. Fang, A. Mehlich, N. Koga, J. Huang, R. Koga, X. Gao, C. Hu, C. Jin, M. Rief and J. Kast, *Nat. Commun.*, 2013, **4**, 2974.

177 L. Fu, L. Li, Q. Bian, B. Xue, J. Jin, J. Li, Y. Cao, Q. Jiang and H. Li, *Nature*, 2023, **618**, 740–747.

178 L. Zeng, M. Song, J. Gu, Z. Xu, B. Xue, Y. Li and Y. Cao, *Biomimetics*, 2019, **4**, 36.

179 Y. Zhang, Y. Wang, Y. Guan and Y. Zhang, *Nat. Commun.*, 2022, **13**, 6671.

180 P. Liu, Y. Zhang, Y. Guan and Y. Zhang, *Adv. Mater.*, 2023, **35**, 2210021.

181 H. Lei, L. Dong, Y. Li, J. Zhang, H. Chen, J. Wu, Y. Zhang, Q. Fan, B. Xue and M. Qin, *Nat. Commun.*, 2020, **11**, 4032.

182 B. Xue, Z. Bashir, Y. Guo, W. Yu, W. Sun, Y. Li, Y. Zhang, M. Qin, W. Wang and Y. Cao, *Nat. Commun.*, 2023, **14**, 2583.

183 T. Wang, Y. Li, J. Wang, Y. Xu, Y. Chen, Z. Lu, W. Wang, B. Xue, Y. Li and Y. Cao, *ACS Biomater. Sci. Eng.*, 2020, **6**, 6800–6807.

184 W. Sun, T. Duan, Y. Cao and H. Li, *Biomacromolecules*, 2019, **20**, 4199–4207.

185 B. Xue, M. Qin, T. Wang, J. Wu, D. Luo, Q. Jiang, Y. Li, Y. Cao and W. Wang, *Adv. Funct. Mater.*, 2016, **26**, 9053–9062.

186 T. J. Hubin and D. H. Busch, *Coord. Chem. Rev.*, 2000, **200**, 5–52.

187 J.-F. Ayme, J. E. Beves, D. A. Leigh, R. T. McBurney, K. Rissanen and D. Schultz, *Nat. Chem.*, 2012, **4**, 15–20.

188 F. B. Cougnon, K. Caprice, M. Pupier, A. Bauzá and A. Frontera, *J. Am. Chem. Soc.*, 2018, **140**, 12442–12450.

189 S. D. Fielden, D. A. Leigh and S. L. Woltering, *Angew. Chem., Int. Ed.*, 2017, **56**, 11166–11194.

190 D. A. Leigh, J.-F. Lemonnier and S. L. Woltering, *Angew. Chem., Int. Ed.*, 2018, **57**, 12212–12214.

191 J.-X. Li, S. Wu, L.-L. Hao, Q.-L. Lei and Y.-Q. Ma, *Sci. Adv.*, 2024, **10**, eadr0716.

192 L. Leibler, M. Rubinstein and R. H. Colby, *Macromolecules*, 1991, **24**, 4701–4707.

193 G. A. Parada and X. H. Zhao, *Soft Matter*, 2018, **14**, 5186–5196.

194 Z. Q. Song, Z. J. Wang and S. Q. Cai, *Mech. Mater.*, 2021, **153**, 103687.

195 J. J. Hernandez, S. P. Keyser, A. L. Dobson, A. S. Kuenstler and C. N. Bowman, *Macromolecules*, 2024, **57**, 1426–1437.



196 D. Montarnal, M. Capelot, F. Tournilhac and L. Leibler, *Science*, 2011, **334**, 965–968.

197 D. J. Bischoff, T. Lee, K. S. Kang, J. Molineux, W. O. Parker, J. Pyun and M. E. Mackay, *Nat. Commun.*, 2023, **14**, 7553.

198 M. Kim, C. Lee, K. Jeon, J. Y. Lee, Y.-J. Kim, J. G. Lee, H. Kim, M. Cho and D.-N. Kim, *Nature*, 2023, **619**, 78–86.

199 B. Saccà and C. M. Niemeyer, *Angew. Chem., Int. Ed.*, 2012, **51**, 58–66.

200 A. E. Marras, L. Zhou, H.-J. Su and C. E. Castro, *Proc. Natl. Acad. Sci. U. S. A.*, 2015, **112**, 713–718.

201 A. C. Yu, H. Chen, D. Chan, G. Agmon, L. M. Stapleton, A. M. Sevit, M. W. Tibbitt, J. D. Acosta, T. Zhang and P. W. Franzia, *Proc. Natl. Acad. Sci. U. S. A.*, 2016, **113**, 14255–14260.

202 J. Cao, X. Zhao and L. Ye, *Ind. Eng. Chem. Res.*, 2020, **59**, 10705–10715.

203 J. Li, H. Liu, C. Wang and G. Huang, *RSC Adv.*, 2017, **7**, 35311–35319.

204 Z. Fang, H. Mu, Z. Sun, K. Zhang, A. Zhang, J. Chen, N. Zheng, Q. Zhao, X. Yang, F. Liu, J. Wu and T. Xie, *Nature*, 2024, **631**, 783–788.

205 X. Kuang, J. T. Wu, K. J. Chen, Z. Zhao, Z. Ding, F. J. Y. Hu, D. N. Fang and H. J. Qi, *Sci. Adv.*, 2019, **5**, eaav5790.

206 M. A. Skylar-Scott, J. Mueller, C. W. Visser and J. A. Lewis, *Nature*, 2019, **575**, 330–335.

